THESIS FOR THE DEGREE OF LICENTIATE OF ENGINEERING

On Techno-economic Assessment of a Multi-terminal VSC-HVDC in AC Transmission Systems

WANG FENG

Division of Electric Power Engineering
Department of Energy and Environment
Chalmers University of Technology
Gothenburg, Sweden 2013

On Techno-economic Assessment of a Multi-terminal VSC-HVDC in AC Transmission Systems

WANG FENG

Division of Electric Power Engineering
Department of Energy and Environment
Chalmers University of Technology
SE-412 96 Gothenburg
Sweden
Telephone +46 (0)31-772 1000

Printed by Chalmers Reproservice
Gothenburg, Sweden, 2013

To my family

Abstract

The Voltage Source Converter based Multi-Terminal high voltage Direct Current transmission system (VSC-MTDC) is currently considered as an attractive technical option for increased transmission capacity and improved controllability and flexibility of an electric power grid, thanks to its unique performance characteristics, and the possibility of using the extruded XLPE cables. In the planning process of embedding a VSC-MTDC system into an ac transmission grid, one must assess the potential values in terms of improved energy efficiency, i.e., reduction of power losses and generation costs. This economic assessment will be a determining feasibility factor of such an option.

Towards this end, this thesis proposes a Mixed ac/dc Optimal Power Flow model (M-OPF) where the traditional ac OPF model is extended to incorporate a detailed steady-state VSC-MTDC system model. In the M-OPF model, the power flow equations of both ac and VSC-MTDC systems are solved simultaneously, and the fundamental technical limits of VSC (the maximum VSC valve current and the maximum dc voltage) are used as operation constraints of VSC stations. A cost-benefit approach using the M-OPF model as the calculation "engine" is proposed to determine the preferred VSC-MTDC alternatives in the transmission expansion planning process. In this approach, the operational benefits from using VSC-MTDC systems are evaluated against their investment costs to derive the Benefit-to-Cost Ratios (BCR) which reflect the cost-effectiveness of the alternatives.

Case studies are conducted using the Nordic 32-bus system to investigate the capability of the VSC-MTDC system in reducing the generation costs and the power losses. The results of these case studies have revealed that the magnitudes of these reductions are very much dependent on the configuration and location of the embedded VSC-MTDC system. The reduction of the generation costs is mainly due to the fact that the VSC-MTDC system enhances transmission capacity by its capability of providing controlled reactive power support and mitigating heavily loaded ac transmission lines. The reduction of the power losses is a trade-off result between the reduced transmission losses by using VSC-MTDC system and the extra power losses introduced by VSC stations. A long-term transmission expansion planning exercise is also conducted using the same study cases to identify the preferred VSC-MTDC alternatives based on the calculated BCR values of all VSC-MTDC alternatives. The study results show that the alternatives with high benefits may not necessarily have high BCRs when the investment costs are considered.

Keywords

AC/DC system, Cost minimization, Cost-benefit analysis, Electric power system, Loss minimization, Multi-terminal VSC-HVDC, Optimal power flow, Transmission expansion planning, Transmission Grid.

Acknowledgement

The financial support from the Chalmers Energy Initiative (CEI) and SP Technical Research Institute of Sweden are gratefully appreciated. I would like to thank all members of the reference group, Claes Breitholtz, Per Norberg, and Sebastien Gros from Chalmers, Bertil Berggren and Lennart Harnefors from ABB, Erik Thunberg and Johan Setréus from SvK, Nayeem Ullah and Emil Hillberg from STRI, for their support of this study.

I would like to thank my examiner and supervisor Lina Bertling Tjernberg, and co-supervisors Tuan A. Le, Anders Mannikoff, Anders Bergman for their encouragement, support and discussion. Abdel-Aty Edris as an international co-advisor from Quanta Technology, USA, is appreciated for supporting me in the research and paper writing.

Working at the division of electric power engineering has been an exciting experience. I would like to thank all colleagues for making this such a nice environment to work in. I would like to specially thank Mebtu Bihonegn Beza and Gustavo Pinares. Your support and discussions during the years have been extremely helpful.

Finally, I want to thank my family. Thank you for support, consideration, patience and endless love. Special thanks to my wife for your support and accompany in these years. You give me courage to restart my study after leaving campus many years!

Wang Feng

2013-07-10

Table of Contents

List of Abbreviations

The following list presents abbreviations that are used throughout this thesis:

AC	Alternating Current
APC	Active Power Control
CSC-HVDC	Current Source Converter based High Voltage Direct Current
DC	Direct Current
GTO	Gate Turn-Off Thyristor
HVDC	High Voltage Direct Current
LCC-HVDC	Line Commutated Converter based High Voltage Direct Current
IGBT	Insulated Gate Bipolar Transistor
MMC	Modular Multi-level Converter
M-OPF	Mixed ac/dc OPF model
MTDC	Multi-Terminal HVDC
NLP	Non-Linear Programming
NPC	Neutral Point Clamped converter
OPF	Optimal Power Flow
PCC	Point of Common Connection
PINT	Put IN one at the Time
PLL	Phase Locked Loop
PWM	Pulse-Width Modulation
RPC	Reactive Power Control
SHE	Selective Harmonic Elimination
TOOT	Take Out One at the Time
TSO	Transmission System Operator
VSC	Voltage Source Converter
VSC-HVDC	VSC based HVDC
VSC-MTDC	Multi-Terminal VSC-HVDC

List of Nomenclatures

The following list presents nomenclatures that are used throughout this thesis:

Constants

A_{ci}	Cost coefficient of generator *i* ($).
A_{li}	VSC loss coefficient of VSC *i* (p.u.).
B_r	Susceptance of VSC phase reactor (p.u.).
B_{ci}	Cost coefficient of generator *i* ($/MWh).
B_f	Susceptance of VSC filter (p.u.).
B_{ij}	Susceptance element of ac network admittance matrix (p.u.).
B_{li},	VSC loss coefficient of VSC *i* (p.u.)
C_{ci}	Cost coefficient of generator *i* ($/MW^{2}h)
C_{li}	VSC loss coefficient of VSC *i* (p.u.).
$g_{i_{dc}j_{dc}}$	Conductance of dc cable i_{dc}-j_{dc} (p.u.).
g_{ij}	Conductance of ac transmission line *i- j* (p.u.).
$G_{i_{dc}j_{dc}}$	Conductance element of dc network admittance matrix (p.u.).
G_{ij}	Conductance element of ac network admittance matrix (p.u.).
k_Q	VSC reactive power lower limit factor.
k_v	Voltage relationship factor between VSC ac and dc buses.
Inv	Investment of VSC-MTDC system (M$).
P_{di}	Active load at bus *i* (p.u.).
Q_{di}	Reactive load at bus *i* (p.u.).
r	Discount rate (%).
R_r	Resistance of VSC phase reactor (p.u.).
R_{tr}	Resistance of VSC transformer (p.u.).
S_{base}	System base value of power (MVA).
S_{nom}	Nominal rating of VSC station (MVA).
t	Operation hours of each period.
V_{dcnom}	Nominal dc bus voltage (kV).
X_r	Reactance of VSC phase reactor (p.u.).
X_{tr}	Reactance of VSC transformer (p.u.).

Variables

BCR	Benefit-to-cost ratio.
Cost	Total generation cost (M$).
$C_1^{yr.p}$	Generation cost of the base case for period *p* and year *yr* (M$).
$C_2^{yr.p}$	Generation cost of the case with VSC-MTDC for period *p* and year *yr* (M$).
I_{vi}	Phase current of VSC valve of VSC *i* (p.u.).
$L_1^{yr.p}$	Power losses of the base case for period *p* and year *yr* (MW).
$L_2^{yr.p}$	Power losses of the case with VSC-MTDC for period *p* and year *yr* (MW).

P_{acloss} Total active losses of ac transmission lines (p.u.).
P_c Active power at VSC ac bus (p.u.).
P_{cdc} DC power at VSC dc bus (p.u.).
P_{dcloss} Total active losses of dc cables (p.u.).
P_{gi} Active power output from generator i (p.u.).
$P_{i_{dc}}, P_{j_{dc}}$ DC power at dc bus i_{dc}, j_{dc} (p.u.).
$P_{i_{dc}j_{dc}}$ DC power flow of dc cable i_{dc}-j_{dc} (p.u.).
P_{loss} Total active losses of the whole system (p.u.).
P_{pcc} Active power at PCC bus (p.u.).
$Pr^{yr.sn}$ Estimated power price within period p and year yr. (M$/MWh).
$P_{vscloss}$ Total active losses of VSCs (p.u.).
PVF^{yr} Present value factor of year yr.
Q_c Reactive power at VSC ac bus (p.u.).
Q_{gi} Reactive power output from generator i (p.u.).
Q_{pcc} Reactive power at PCC bus (p.u.).
S_c Apparent power at VSC ac bus (p.u.).
S_{ij} Power flow of ac transmission line i- j (p.u.).
TB Total economic benefit (M$).
V_c Voltage magnitude at VSC ac bus (p.u.).
V_{cdc} DC Voltage at VSC dc bus (p.u.).
V_f Voltage magnitude at VSC filter bus (p.u.).
V_i, V_j Voltage magnitude at ac bus i and j (p.u.).
$V_{i_{dc}}, V_{j_{dc}}$ Voltage magnitude at dc bus i_{dc} and j_{dc} (p.u.).
V_{pcc} Voltage magnitude at PCC bus (p.u.).
δ_c Voltage angle at VSC ac bus (degree).
δ_f Voltage angle at VSC filter bus (degree).
δ_i, δ_j Voltage angle at ac bus i and j (degree).
δ_{pcc} Voltage angle at PCC bus (degree).

Indices

i, j Index of ac bus, generator, VSC station.
i_{dc}, j_{dc} index of dc bus.
p Index of operation period.
yr Index of year.

Sets

N Set of all ac buses.
NG Set of all generators.
NL Set of all loads.
M Set of all dc buses.

Variable limits

$\underline{a}$, $\overline{a}$ Lower and upper limits of the variable a (variable a can be voltage V, active power P, reactive power Q, etc.).

Chapter 1

Introduction

This chapter presents a short introduction of High Voltage Direct Current (HVDC) technology, including both the Current Source Converter based HVDC (CSC-HVDC) and Voltage Source Converter based HVDC (VSC-HVDC). Their technical characteristics are compared. The motivation and main contribution of the thesis are highlighted. The organization of the thesis is introduced. The publications are listed at the end of the chapter.

1.1 Historical Background of HVDC

The first commercial HVDC project in the world was put into operation in 1954 to transfer 20 MW electric power with 100 kV direct voltage from the mainland of Sweden to the Gotland island using submarine cables. It used the mercury-arc valves to convert the electric power between ac and dc forms [1]. Since then, the HVDC technology has been developed dramatically. The mercury-arc valves were replaced by thyristor valves in the 1970s. The ratings of HVDC projects have been gradually increased to 7200 MW with direct voltage ±800 kV in the Jinping-Sunan HVDC project in China [2]. This type of HVDC technology is called Current Source Converter based HVDC (CSC-HVDC) because it is shown as a current source to the grid. It is also called Line Commutated Converter based HVDC (LCC-HVDC) since thyristors employed as switching devices in the converter can only be turned off when the current through it passes zero, therefore, it requires line voltage for commutation.

Since 1990s, a new type of HVDC technology mainly using self-turn-off devices, such as Insulated Gate Bipolar Transistor (IGBT), has been developed and applied in the electric power system. It is called Voltage Source Converter based HVDC (VSC-HVDC) since it can be considered as a voltage source when connected to the grid. The first VSC-HVDC test system was field demonstrated in 1997 in Hellsjön, Sweden. Then the first commercial project was put into operation also in Gotland, Sweden, in 1999 [3]-[5]. Many VSC-HVDC projects have been put into operation or are in planning for the near future.

Today, the HVDC technology can generally be categorized in these two types

(CSC- and VSC-HVDC) based on the switching devices employed in the converter. Thyristor valves are still used in CSC-HVDC projects, while IGBTs are commonly employed in VSC-HVDC projects, even though application of other power electronic devices, e.g., Gate Turn-off Thyristor (GTO), is reported in a few test projects [6]. Some of the main characteristics of CSC- and VSC-HVDC are listed and compared in Table 1.1.

Table 1.1. Comparison of CSC- and VSC-HVDC

Items	**CSC-HVDC**	**VSC-HVDC**
Highest rating	7200 MW, ±800 kV (Using overhead line) [2]	1200 MW, ±320 kV (Using cable) [7]
Average power losses of one converter station	About 0.75 %	About 1 % [8]
Switching frequency	50 or 60 Hz, the grid frequency	More than 1000 Hz for PWM
Independent control of active and reactive power	No	Yes
Reactive power support	Supplied by shunt capacitor banks	Supplied by VSC itself
Supply to passive networks	No	Yes
Power flow direction reverse	Keep direct current direction constant, and change direct voltage polarities of two poles	Keep direct voltage polarities constant, and reverse the direct current direction
Multi-terminal configuration	System with three-terminals is in operation. [9]	Theoretically, no limitations (under research and development)

As can be seen from Table 1.1, the CSC-HVDC has much larger power rating than that of VSC-HVDC, which makes it suitable for the high voltage bulk power transmission over long distance. A recent example is the Jinping-Sunan HVDC project in China as mentioned above. VSC-HVDC can be used for the integration of renewable power generation, and supplying power to passive networks. Embedding VSC-HVDC in an ac grid results in additional controllability and flexibility in the operation of the ac grid [10], [11]. However, due to the lower voltage and current ratings of the IGBTs and the relatively higher losses of the VSCs make VSC-HVDC applicable for much lower power rating compared to the CSC-HVDC, which is currently used in the bulk power transmission applications.

The multi-terminal HVDC (MTDC) system was first developed in the 1980s in the Italy–Corsica–Sardinia HVDC project [12]. Another MTDC system is the Quebec–New England project [9], transferring hydro power from Canada to USA. Both of these MTDC systems are CSC-HVDCs. However, the application of MTDC system using CSCs is, technically and operationally, limited because the direct current is always flowing in one direction between two converter terminals.

Reversing the direction of the dc power flow between any two terminals can only be achieved by reversing the polarity of the dc voltage. This implies sophistication in the coordination of control and operation among terminals.

When VSCs are used in the MTDC system, the coordination of control and operation among terminals will be much easier compared to CSCs because the dc power flow is changed by changing the direct current direction and no need to change the polarities of direct voltage. Connecting a new VSC station to an existing VSC-HVDC system is like connecting an ac substation to an ac grid. Some VSC-MTDC projects have been planned or under construction. For example, the "South West Link" project was planned as a three terminal VSC-MTDC system [13], [14], even though its third terminal has been cancelled recently because of market reasons. VSC-MTDC systems connecting offshore wind farms are also proposed and studied, e.g., the offshore dc grid in the North Sea [15], [16].

1.2 Background and Objectives of the Thesis

As introduced in Section 1.1, the VSC-MTDC system has been considered as an alternative in the integration of offshore wind farms and in reinforcement of the aging electric power grid. The main motivation of using VSC-MTDC system in the transmission grid comes from new challenges in the operation and reinforcement of the traditional ac transmission grid. For example, the integration of large-scale renewable power resources increases the uncertainty of power generation; the interconnected electric power market requires more flexible power flow control; and the public pressure due to the environment impact of overhead transmission lines results in difficulties in the reinforcement of the aging transmission infrastructure system [17], [18]. VSC-MTDC has a great positive potential in dealing with these challenges thanks to its specific performance characteristics as shown in Table 1.1 and summarized in [10] and [19], e.g., providing flexibility and controllability in managing active and reactive power flows, and possibility of using extruded XLPE cables. Furthermore, the VSC-MTDC is capable of providing additional controllability in the transmission system. VSC-MTDC system can, therefore, enhance the system operation since it can affect the power flow of the connected ac grid across a much larger area compared to the two-terminal VSC-HVDC system.

When a VSC-MTDC system is considered as an alternative in reinforcement projects of a transmission grid, and is embedded into an existing ac transmission grid, a key issue will be evaluation of its potential contribution in optimizing the operation of the mixed ac/dc grid, e.g., minimizing the generation cost and total system losses. The main objectives of this research reported in this thesis are to develop an approach to evaluate the benefits of using an embedded VSC-MTDC system in an ac grid. Thus, to optimize the transmission expansion planning and the operation of the mixed ac/dc grid based on VSC-MTDC. The current study

focuses on the steady state condition of the electric transmission grid, such as the Optimal Power Flow (OPF) of the mixed ac/dc grid.

1.3 Main Contributions

The main contributions of this research are the following:

a) Extension of the traditional ac OPF to incorporate VSC-MTDC.

b) Evaluation of the benefits of embedded VSC-MTDC systems in generation cost and power loss minimization.

c) Development of a benefit-cost analysis approach for transmission expansion planning to evaluate and compare the economics of different VSC-MTDC system alternatives.

1.4 Organization of the thesis report

The thesis is organized as follows:

- Chapter 1 introduces a historical background of HVDC technologies, the motivation and objectives of this thesis.

- Chapter 2 describes technical details of VSC-MTDC which includes the VSC topologies and modulation, control and operation principles. These details are the foundation of the VSC-MTDC model proposed in Chapter 4.

- Chapter 3 introduces the traditional ac OPF and the transmission expansion planning.

- Chapter 4 presents the extended OPF model incorporating a steady-state model of the VSC-MTDC system.

- Chapter 5 presents the analysis of the capability of the VSC-MTDC system in reduction of system generation cost and power transmission losses.

- Chapter 6 proposes a cost-benefit approach for the evaluation of the effectiveness of using the embedded VSC-MTDC in an existing ac grid.

- Chapter 7 concludes the report with final conclusions and future work.

1.5 List of publications

The following papers have been published based on this thesis. The key issues addressed in the papers are summarized in Table 1.2.

[I] F. Wang, L. Bertling, T. Le, A. Mannikoff, and A. Bergman, "An Overview Introduction of VSC-HVDC: State-of-art and Potential Applications in Electric Power Systems," in *Cigrè International Symposium*, Bologna, Italy, Sept. 2011.

[II] F. Wang, T. Le, L. Bertling, A. Mannikoff, and A. Bergman, "A Cost-Benefit Analysis of The Multi-Terminal VSC-HVDC Embedded in an AC Transmission System Using a Proposed Mixed AC/DC Optimal Power Flow," in *10th IEEE International Conference on European Energy Market EEM13*, Stockholm, Sweden, May 2013.

[III] F. Wang, T. Le, L. Bertling, A. Mannikoff, and A. Bergman, "A Mixed AC/DC OPF Incorporating Multi-Terminal VSC-HVDC and its Application on Transmission Loss Minimization," in *PowerTech 2013*, Grenoble, France, June 2013.

[IV] F. Wang, T. Le, L. Bertling, A. Mannikoff, and A. Bergman, " A New Approach for Benefit Evaluation of Multi-Terminal VSC-HVDC Using A Proposed Mixed AC/DC Optimal Power Flow," Accepted by *IEEE Transactions on Power Delivery, Special Issue: HVDC Systems and Technologies*, May 2013.

Table 1.2. Contents of papers

	Literature review	**M-OPF**	**Generation cost analysis**	**Power loss analysis**	**Cost-benefit approach**
[I]	X				
[II]	X	X	X		X
[III]	X	X		X	
[IV]	X	X	X	X	X

Chapter 2

VSC-HVDC Technologies: State-of-the-Art

This chapter reviews technical details of VSC-HVDC (including VSC-MTDC), e.g., system configuration, VSC topologies and modulation methods, control and operation principles. These technical details are the foundation of the VSC-MTDC steady-stage model, which will be presented in Chapter 4.

2.1 Configuration and Station Equipment

2.1.1 Configuration of VSC-HVDC

The configuration of a VSC-HVDC system can generally be divided into two types, symmetric configuration and asymmetric configuration [7]. Figure 2.1 depicts these two configurations.

Symmetric configuration is a commonly used configuration of VSC-HVDC system as show in Figure 2.1. In this configuration, the midpoint of the dc side of the converter is grounded, and two poles connecting to the converter transmit balanced power with the same direct voltage magnitude but opposite voltage polarities.

Asymmetric configuration is introduced recently for VSC-HVDC system by adopting some advantages of bipolar configuration of CSC-HVDC system [7]. In this configuration, two converters are connected in series at one station, and the connection point is grounded. Therefore, the dc side of each converter has asymmetric direct voltage, from zero to positive or negative direct pole voltage. Two converters can be operated separately. Therefore, the whole VSC-HVDC system can be operated in either bipolar or monopolar configuration, which increases the reliability of power transmission.

2.1.2 Station Equipment

The following equipment may be included in a VSC-HVDC system based on the

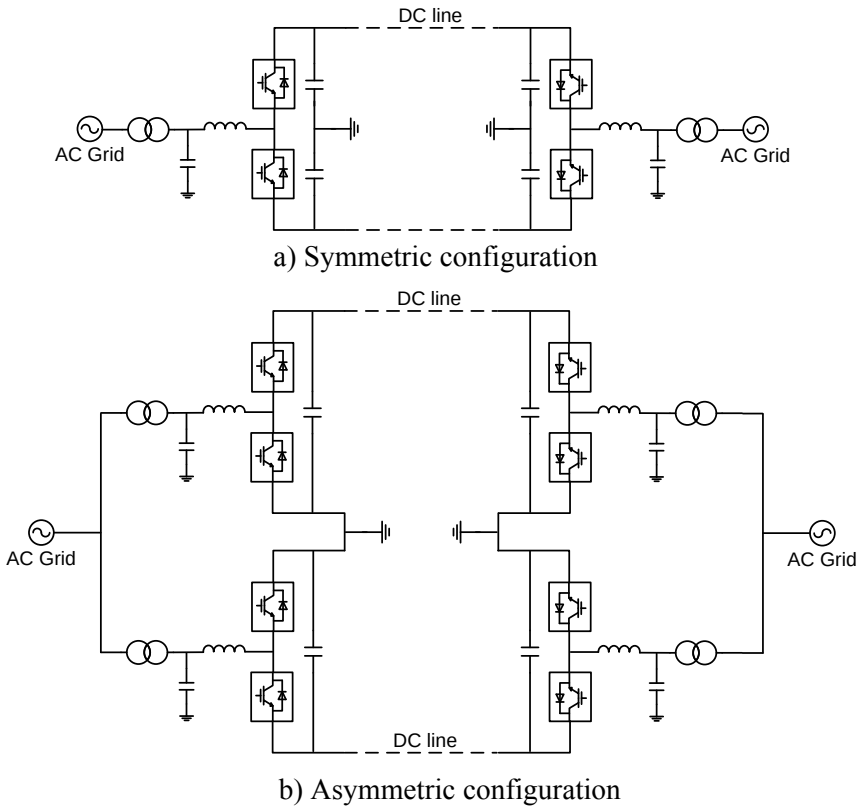

Figure 2.1 Configuration of VSC-HVDC system: a) Symmetric; b) Asymmetric.

VSC types:

- VSCs are the core component of VSC-HVDC, which convert the power between ac and dc forms.

- Phase reactors reduce the harmonic contents of the ac voltage generated by a VSC. Meanwhile, it also supplies the control of active and reactive power, which will be described in Section 2.3.

- AC filters provide the high-pass filter of the ac voltage for the harmonic components because of the switching operation of IGBTs.

- Transformers are used to connect the VSC and ac grid. The on-load tap changer is usually equipped to adjust the voltage at the filter bus within the required range.

- DC capacitors provide a low inductive path for the turned-off current when IGBTs are operated. Meanwhile, they store energy for the dc voltage control. When more energy is stored, the dc voltage is higher, and vice versa.

- DC cable used for VSC-HVDC is an extruded polymer insulated type, which is light and oil free compared with e.g., traditional oil paper insulation cables.

Other equipment used in a VSC station could be: ac breakers, measurement devices, cooling system, etc. Detailed description of equipment for VSC-HVDC can be found in [7], [19].

It should be noted that when Multi Modular Converter (MMC) is used, the ac filter may not be needed because the ac voltage wave form generated by VSC could be very close to a sinusoidal wave form [20].

2.2 Topology and Modulation of VSC

2.2.1 VSC Topologies

The two-level converter with the Pulse Width Modulation (PWM) method is the first type of voltage source converter used in the electric power system, shown in Figure 2.2. Two-level means that the alternating voltage generated by VSC at its ac terminal has two voltage levels, positive and negative direct voltages, because of the switching operation. The typical two-level converter uses series-connected IGBTs as the switch device to share the high blocking voltage. Anti-parallel freewheeling diodes ensure four-quadrant operation of the converter.

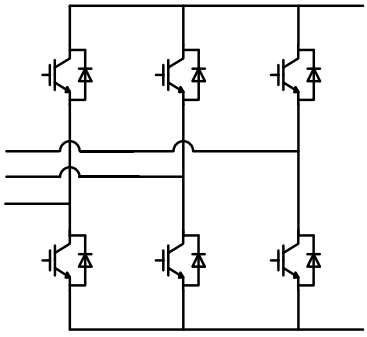

Figure 2.2. Topology of a two-level converter.

The two-level converter has a simple topology compared to other VSC types, e.g., three-level converter. However, its major drawback is the high power loss due to the high switching frequency using PWM. In order to reduce the VSC losses, many other VSC topologies are proposed, especially multilevel topologies [21], [22]. Multilevel means that more than two voltage levels can be obtained. Take a three-level diode-clamped Neutral-Point-Clamped (NPC) converter [23] as an example, shown in Figure 2.3, it supplies one more voltage level by adding two grounded clamping diode on the basis of two-level topology. Because each phase of the converter has three voltage levels, positive dc terminal, negative dc terminal, and the intermediate dc voltage, the alternating voltage wave shape is closed to a

sinusoidal. Therefore, the total harmonic content and switching losses will be decreased. This feature further benefits the required ac filter rating. Theoretically, a higher number of voltage levels will further help in the harmonic and switching loss reduction. But converters with more than three levels are not considered in the HVDC application because of certain engineering reasons, such as insulation and cooling problems [24].

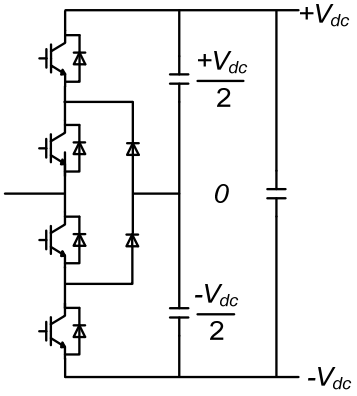

Figure 2.3. One phase of a three-level NPC.

A new VSC topology, Modular Multilevel Converter (MMC) using cascaded connection logic, is developed [25]-[27] and applied recently in VSC-HVDC projects [20]. Compared with the other types of multilevel converters, the MMC does not have a common capacitor connecting dc buses. Different types of modules are used in MMC. Figure 2.4 shows the MMC with half-bridge module [28] and full-bridge module [29]. The operation principle of MMC with the cascaded connection method is explained below using half-bridge module type as an example. Each half-bridge module consists of two valves and can be switched in three modes as described below:

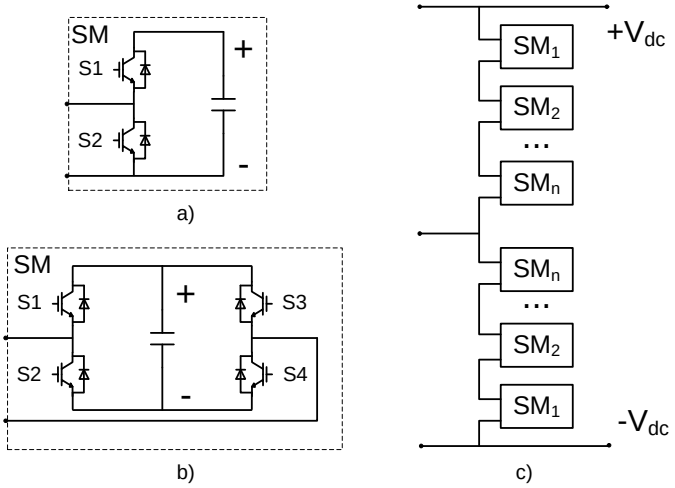

Figure 2.4. Modular multilevel converter topology: a) half bridge module, b) full bridge module, c) one phase of a MMC.

1) When S1 is turned on and S2 is turned off, the capacitor is inserted into the circuit. The module contributes with voltage to the phase voltage.

2) When S1 is turned off and S2 is turned on, the capacitor is bypassed.

3) When S1 and S2 are both turned off, the module is blocked when the capacitor voltage is higher than outside voltage.

Compared to the half-bridge module, the full-bridge module can supply extra flexibility in operating VSC. For example, the fault current in the dc side can be cut off by turning off all the IGBTs [30], [31]; the dc voltage can be quickly switched to zero by shifting the voltage polarity of a module opposite to adjacent ones, etc. However, more IGBTs are needed for the full-bridge module, which increases the device cost and the switching losses in the normal operation mode.

MMC is an attractive topology for HVDC application. The cascaded connection method permits each module, theoretically, to switch on and off only once per period. Thus, the switching losses are greatly reduced. On the other hand, the output waveform is function of the number of the cascaded modules. For example, 200 cascaded modules are used in each converter arm of a 400 MW MMC [32]. This results in a very small harmonic content of the voltage, meaning that it is not necessary to include an ac filter in a HVDC station. Line to neutral voltage waveforms of two-level converter, three-level converter, and MMC are shown in Figure 2.5.

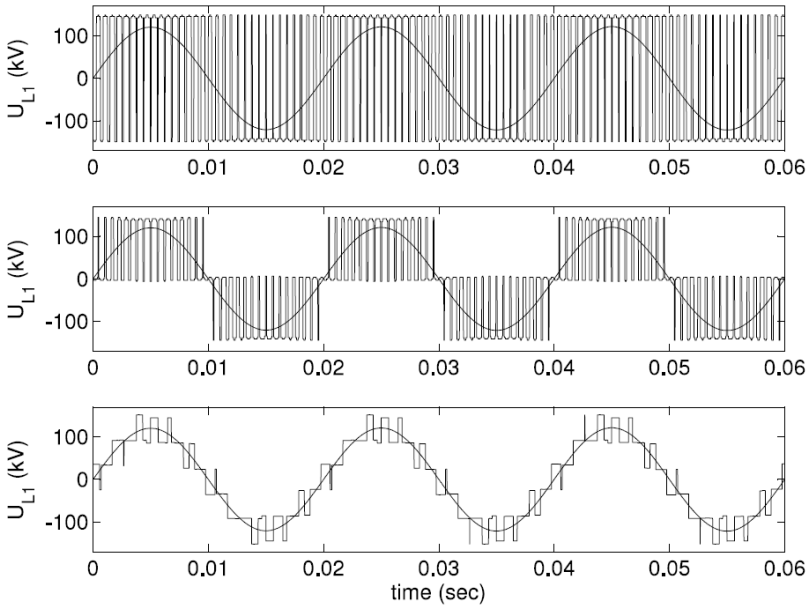

Figure 2.5. Line to neutral voltage waveform of three converters types: (Upper) Two-level converter, (Middle) Three-level converter, (Lower) MMC [24].

2.2.2 Modulation Methods

Pulse-Width Modulation (PWM) is the basic modulation method of VSC [33]. By comparing a reference sinusoidal voltage waveform to a saw tooth waveform, IGBTs can be controlled to switch on or off at the right instant, and the voltage output is therefore generated at the VSC ac terminal bus, which contains the fundamental frequency from the reference voltage waveform and much higher frequency harmonics. After an ac filter, the high frequency harmonic is removed and the desired sinusoidal voltage is obtained. Figure 2.6 shows these voltage waveforms. By changing the magnitude and phase angle of the reference voltage waveform, the magnitude and phase angle of the VSC ac voltage output will be changed correspondingly.

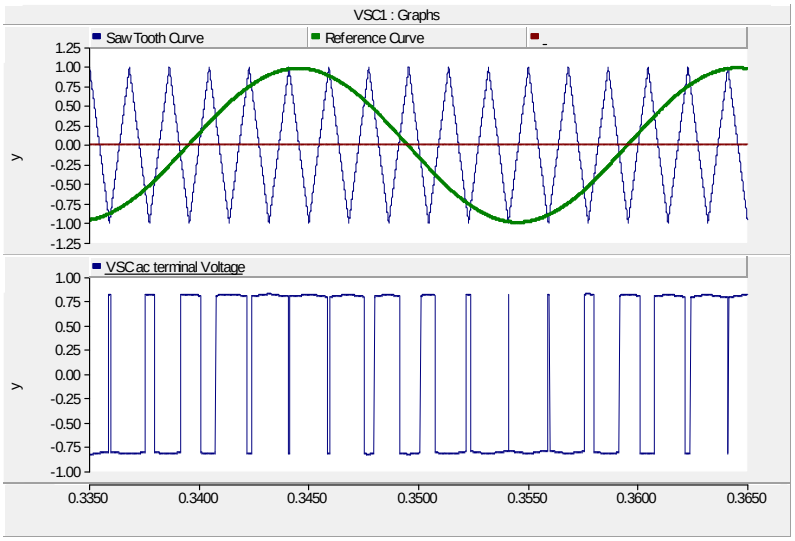

Figure 2.6. Waveforms of PWM.

When a VSC is used in the electric power system, it usually works in an under modulation condition to avoid high harmonic components [33], i.e., the peak value of the sinusoidal reference voltage is not higher than the peak value of the saw tooth curve. However, the VSC cannot fully utilized the dc voltage to generate the sufficient ac voltage at the grid side by using the under modulation method [33], [34]. In order to improve the output voltage, the third harmonic is injected into the fundamental voltage as the reference voltage waveform, and 15 % higher ac voltage output can be expected compared to the normal PWM method [33]-[35]. Meanwhile, the third harmonic is not transferred to the ac grid when the transformer is delta connected. For multi-level converter or MMC, the Selective Harmonic Elimination (SHE) is an effective method to reduce the total harmonic distortion [36]-[40]. If IGBTs is switched on or off at specific instant, a specific harmonic can be eliminated, which benefits the rating of required ac filter. Moreover, the power loss because of harmonics will be reduced by using SHE, which contributes to the reduction of the VSC total power loss.

2.3 Modeling, Control, and Operation of VSC-HVDC

2.3.1 Modeling of VSC

A large number of papers can be found about the modeling and control of VSC-HVDC from different points of view, some of which are in [41]-[46]. Generally, the VSC can be treated as an equivalent ideal voltage source seen from the ac grid side, and an equivalent current source seen from the dc side as shown in Figure 2.7. The VSC control system has the freedom to specify the magnitude, phase, and frequency of the produced ac voltage at the VSC ac terminal, while the dc voltage can be controlled at the dc side. Although various topologies are proposed, a VSC can always be treated as an equivalent ideal voltage source seen from the ac grid side, no matter which topology is used. Certainly, it should be noted that the ideal voltage source model may not be detailed enough for the fast transients, e.g., electromagnetic transient study types, which requires a more detailed modeling of the VSC.

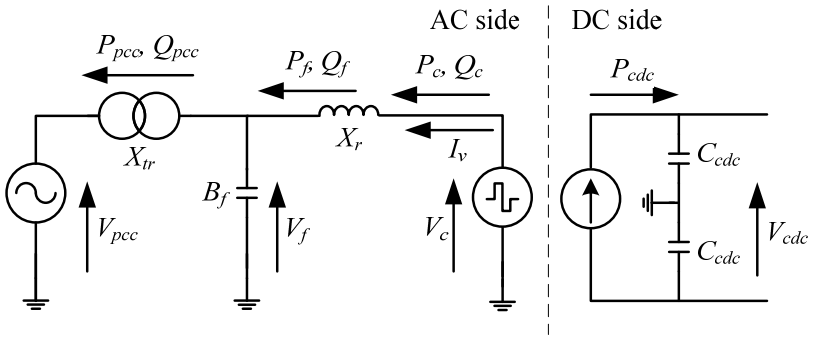

Figure 2.7. Equivalent voltage and current source model of VSC.

When a VSC connects to an ac grid via phase reactors, the VSC, phase reactors, and the ac bus at grid side can be considered as an equivalent two-port ac transmission network as shown in Figure 2.8. The active and reactive power injection to the ac grid bus can be calculated by Eq. (2-1) and (2-2) when only the voltage and current of fundamental frequency are considered.

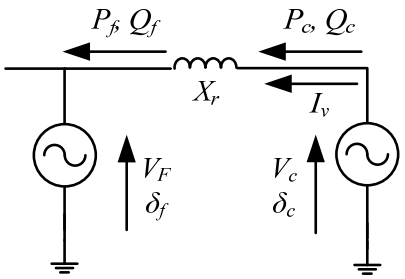

Figure 2.8. Equivalent two-port transmission network at VSC ac side.

$$P_f = \frac{V_c V_f \sin\left(\delta_c - \delta_f\right)}{X_r} \tag{2-1}$$

$$Q_f = \frac{V_c V_f \cos\left(\delta_c - \delta_f\right) - V_f^2}{X_r} \tag{2-2}$$

2.3.2 Control of VSC

From Eq. (2-1) and (2-2), a basic control method of VSC can be obtained: the active and reactive power injection from VSC to the ac grid can be controlled by controlling the magnitude and phase angle of the VSC output voltage at the ac terminal. This control method is called voltage-angle control or power-angle control [47], [48]. Figure 2.9 shows the structure of the voltage-angle control method. Three variable, (voltage magnitude, phase angle, and frequency) are controlled separately by three controllers, Reactive Power Controller (RPC), Active Power Controller (APC), and Phase Lock Loop (PLL).

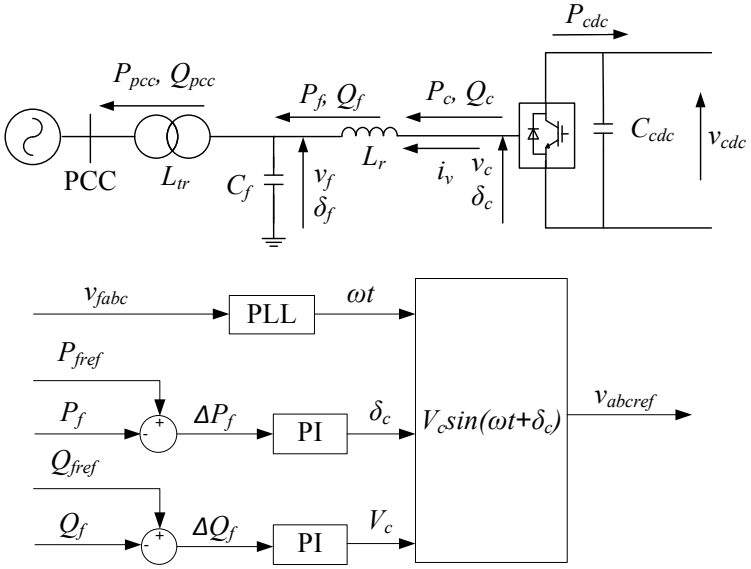

Figure 2.9. Block diagram of the power-angle control.

Another control method in the VSC-HVDC application is the vector current control [49]-[51]. Its basic principle is to independently control the active and reactive power injection from the VSC to the ac grid by controlling the decoupled current vector of the phase reactors in a d-q frame. The structure of the vector current control is shown in Figure 2.10. A PLL is used to align the d-q frame with the grid voltage in order to synchronize the VSC to the ac grid. Compared to the voltage-angle control method, vector current control can limit the valve current during a fault. Thus, valves are protected from high fault current, and converter block can be avoided.

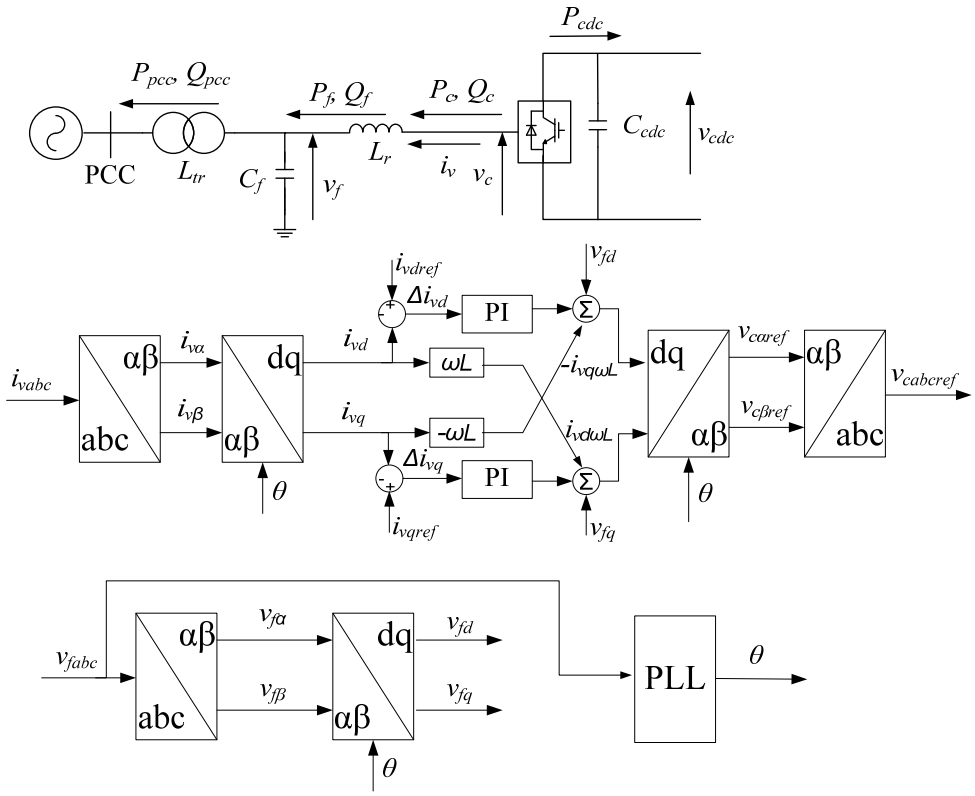

Figure 2.10. Block diagram of the vector current control.

Besides the controllers described in the above, some controllers are used to complement other VSC control functions. An unbalanced current control method is reported to work under unbalanced network condition in [52] by combining two controllers in both positive and negative d-q frames. Reference [45] studied the power-frequency control mode when a VSC is connected to an islanded network.

The hierarchical structure of the control system is usually used in the commercial VSC-HVDC project. The whole control system of VSC is split into different layers with different control blocks to perform different control functions. A typical control system introduced in [53] consists of three layers: converter control layer, auxiliary control layer, and system control layer. Figure 2.11 shows the structure of the whole control system. The core part of the converter control layer is the inner current control assisted by other foundational control functions, such as the ac/dc voltage control. The functions of this control layer ensure smooth operation of the converter by receiving power/voltage order references from operators and supplying correct reference voltage to the converter. The application control layer includes the control functions of power flow control, reactive power control, frequency control, and so on. The operation mode of converters will be determined by this layer. The system layer controllers establish the functions for achieving bulk electric grid objectives, such as the power flow control, congestion management, and voltage support.

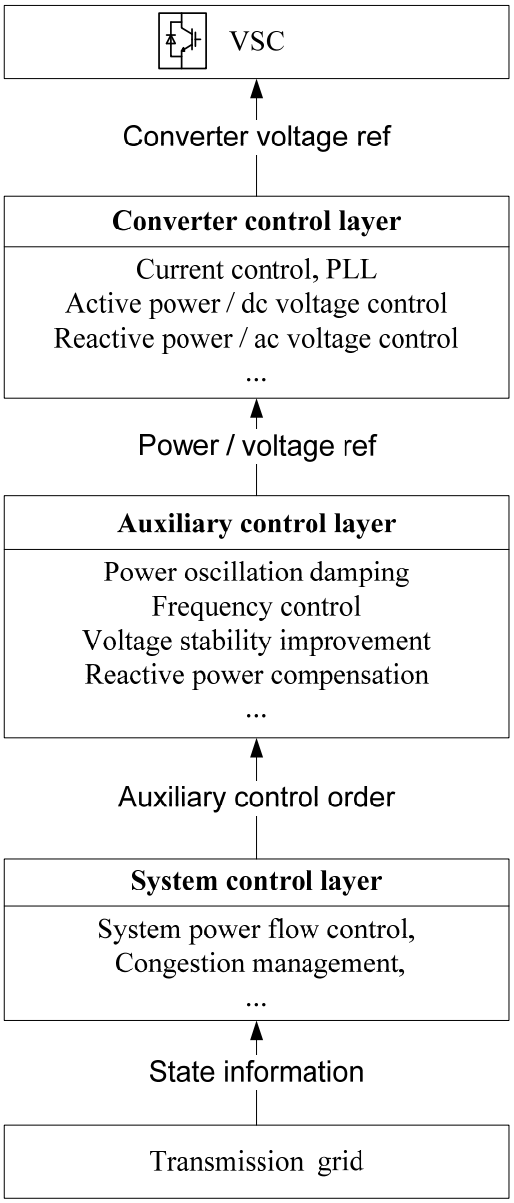

Figure 2.11. Hierarchical control system structure of VSC.

2.3.3 Operation of VSC-HVDC

When two VSC stations are connected via cables or overhead lines to form a VSC-HVDC system, the operation coordination between two VSC stations is necessary. Generally, the basic operation principle of a two-terminal VSC-HVDC system is to keep the power balance between two VSC stations, and to keep the direct voltage as high as possible within accepted limits to minimize the transmission loss through the dc links. Usually, one VSC station controls the dc voltage and the other VSC station controls the active power injection to the ac grid. The reactive power injection/absorbed between the VSC stations and the ac grid can be controlled independently at the two VSC stations [19]. If necessary, the

frequency of the ac grid can be controlled instead of the active power, and the reactive power control can be replaced by ac voltage control [54].

The normal operation of the VSC is, in principle, constrained by the maximum current through VSC valves and the maximum dc voltage [19], [55]. The former determines the maximum VSC apparent power limit, and the latter defines the VSC reactive power output limit. Usually, the VSC active and reactive power outputs are controlled on the Point of Common Connection (PCC) bus or the ac filter bus. The operation constraints of VSC are also applied on these two buses. Take ac filter bus as an example, the constraints are formed by Equations (2-3) and (2-4) if the resistances of phase reactors are neglected. Figure 2.12 shows the VSC operation area with capability limits.

$$\left|S_f\right| \le \left|V_f \overline{I}_r\right| \tag{2-3}$$

$$Q_f \le B_r \left(V_f^2 - V_f V_c e^{j\left(\delta_f - \delta_c\right)} \right) \tag{2-4}$$

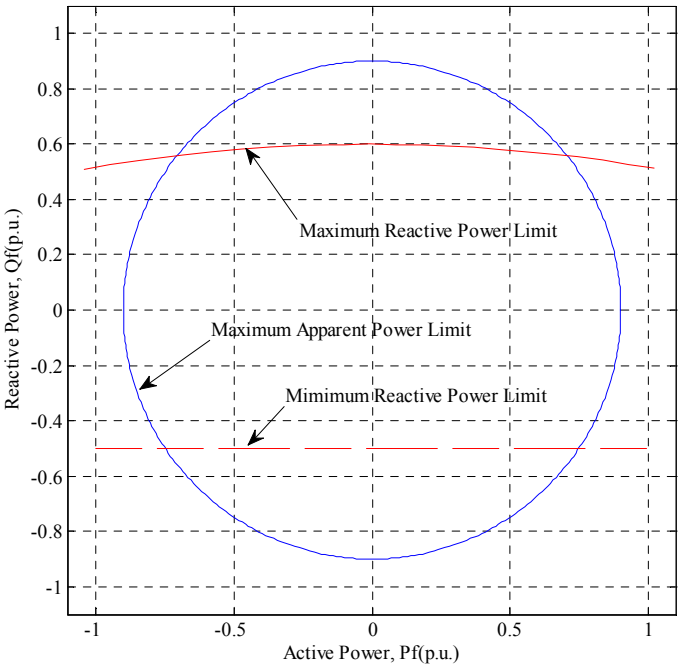

Figure 2.12. Operation area of VSC with limitations.

2.4 Control and Operation of VSC-MTDC

An example of a considered three-terminal VSC-HVDC system is shown in Figure 2.13. Three ac grids are connected by three VSC stations and two dc links.

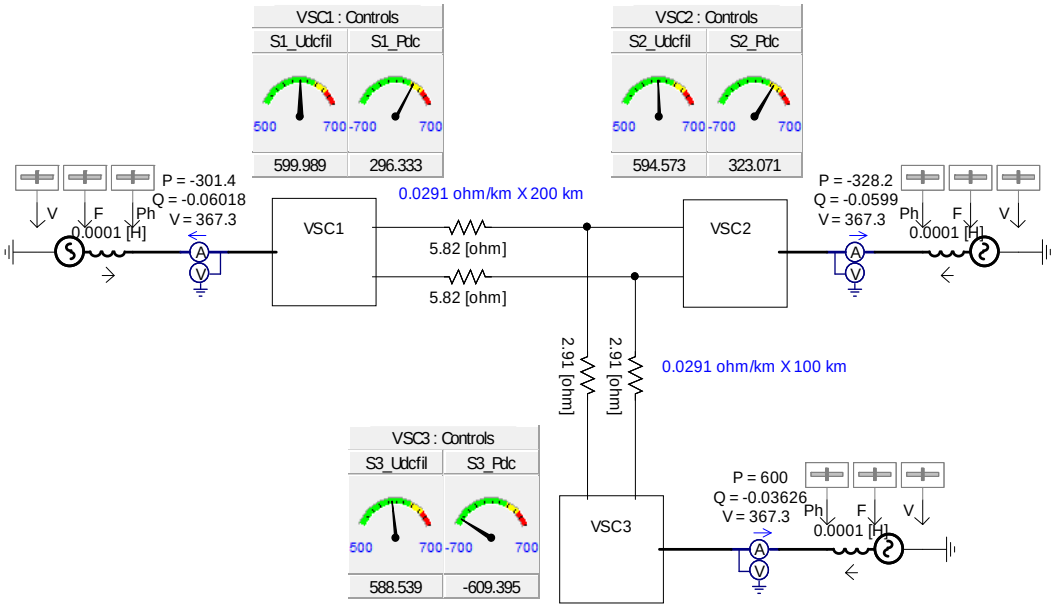

Figure 2.13. Configuration of a three terminal VSC-HVDC system.

The operation principle of a two-terminal VSC-HVDC system described in Section 1.3 is also suitable to the VSC-MTDC system. However, two basic questions shall be considered since the dc power flow within the VSC-MTDC system is more complicated than that of the two-terminal VSC-HVDC system. One question is how to keep the power balance among all dc terminals, and the other question is how to keep the direct voltage at all terminals within limits. Therefore, one more control function is needed for the VSC-MTDC system to coordinate the power exchange of all terminals in order to keep the power balance and compensate system losses.

A voltage margin control is proposed in [6] and [16], which is shown in Figure 2.14. The basic idea of the voltage margin control is that one VSC station controls the direct voltage, and all other VSC stations control the power exchange with a certain freedom of dc voltage variation at their own terminal. The VSC station regulating the dc voltage has to compensate the unbalanced power exchange of all other VSC stations and the overall dc power losses. However, during a fault period, the unbalanced power exchange may be far beyond the direct voltage control ability of each VSC station, and the direct voltage may not be controlled any more.

In order to strengthen the dc voltage control ability, the voltage droop control is proposed [56], [57] as shown in Figure 2.15. By applying a voltage-power droop in more than one VSC station, these stations share the total unbalanced power exchange and system losses on the basis of the predefined droop characteristic. Therefore, the dc voltage control ability is greatly improved [58], [59].

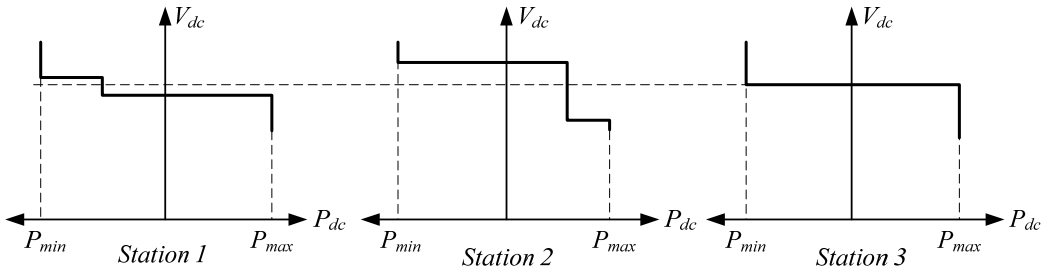

Figure 2.14. Principle of voltage margin control.

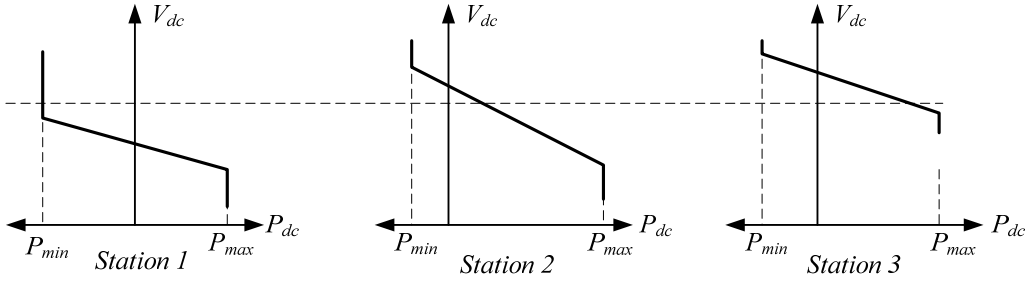

Figure 2.15. Principle of voltage droop control.

A combination of the voltage margin control and voltage droop control together in order to get better performance is presented in [60]. The proposed voltage-power characteristic is shown in Figure 2.16.

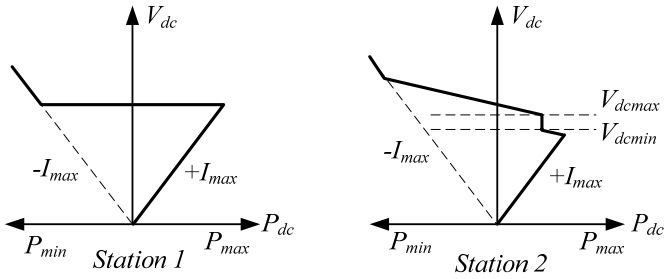

Figure 2.16. Modified voltage droop control.

2.5 Real Project Examples

Information of VSC-HVDC projects can be found in the list [61] and [62], prepared by IEEE Transmission and Distribution Committee. Some selected examples are shown in Appendix A. These projects reflect the development of VSC-HVDC technology. The power rating increases from less than 100 MW to more than 1000 MW, and the dc voltage level increases from 10kV to 320 kV for dc cables, and 350 kV for overhead lines. All these improvements are the results of the development of the power electronic switching devices, VSC topologies, and control methods

.

Chapter 3

Brief Review of Optimal Power Flow and Transmission Expansion Planning

This chapter reviews the background of Optimal Power Flow (OPF) and transmission expansion planning practices. The definition and solution of OPF is described. State-of-the-art of transmission expansion planning, and the application of cost-benefit analysis in transmission expansion planning are introduced.

3.1 Optimal Power Flow

Optimal Power Flow (OPF) has been developed since 1962 in order to find the optimal solution of the economic dispatch of electric power system [63]. The basic principle of OPF problem is to minimize (or maximize) an objective function by finding the "best" system state and variable values with respect to operational or physical constraints. For example, the system total generation cost can be minimized by adjusting the generator power output and other controllable variables to a certain value [64]. Nowadays, OPF is commonly used in the operation and expansion planning of the electric power system as a powerful tool in obtaining optimum system operation states.

3.1.1 Definition and Formulation of Optimal Power Flow

A general OPF model of an ac grid can be stated as below [63] [65]:

$$\text{Minimize } f(x,u) \tag{3-1}$$

Subject to

$$g_{ac}(x,u) = 0 \tag{3-2}$$

$$h_{ac}(x,u) \leq 0 \tag{3-3}$$

$$\underline{u} \le u \le \overline{u} \tag{3-4}$$

where x represent state variables, e.g., ac bus voltage magnitude and angle; u represent decision variables, such as generator active power, generator bus voltage; $f(x, u)$ represent the objective function, e.g., power generation cost and power transmission losses; $g_{ac}(x, u)$ are ac power flow equations; $h_{ac}(x, u)$ represent operational constrains, e.g., currents and voltages limits; $\underline{u}$ and $\overline{u}$ are the physical limits of decision variables.

System generation costs and transmission power losses are two traditional objective functions used for the economic dispatch of the generators, and economic operation of the transmission grid. Other forms of the objective function can also be achieved. For example, the social welfare is usually considered as an objective function in the present transmission expansion planning [66]-[68], the congestion cost is minimized in the network congestion management [69]. Besides the single optimal problem, the multi-objective functions are usually needed in some real-world problems, such as the transmission expansion planning [66], [70]-[72]. The benefits of using multi-objective function include allowing the management and coordination of different objectives, simplifying the decision making process, and supplying indications on the consequences of the decision [73].

Decision variables are system variables controlled by the active devices in an electric power system, e.g., the active power output of generators, the voltages at generator terminals, the tap positions of transformer on load tap changers, etc. Nowadays, more and more power electronic devices are utilized in the electric power system, such as the HVDC and FACTS. They provide more controllability of the system. In other words, they supply more decision variables of OPF. By adjusting these decision variables, an optimized system operation state will be achieved. On the contrary, State variables are usually the bus voltage, transmission line current, etc. All these state variables change with the change of decision variables based on the laws of physics.

Conventional constraints of OPF include two types, equality and inequality constraints. The equality constraints are typically the power flow equations (3-5) and (3-6) [63]. The inequality constrains are usually the operation or physical limits. For example, transmission line capacity is constrained by its thermal limit, and the bus voltages are within their insulation limits, etc. Besides the constraints from the traditional electric power system, other constraints should be included in OPF for specific studies. For example, the voltage or transient stability constraints are necessary when the system is subjected to the risk of voltage instability situations [74]-[79]. When power electronic devices are used in the transmission grid e.g., HVDC and FACTS, the constraints from these devices shall be included in OPF [78], [80]. The OPF incorporating constraints of a VSC-MTDC system will be presented in the following sections. In a deregulated environment, the

model and constraints of the power market are also an important part of OPF.

$$P_{gi} - P_{di} = V_i \sum_{j=1}^{N} \left[G_{ij} \cos\left(\delta_i - \delta_j\right) + B_{ij} \sin\left(\delta_i - \delta_j\right) \right] V_j, \quad \forall i \in N \tag{3-5}$$

$$Q_{gi} - Q_{di} = V_i \sum_{j=1}^{N} \left[G_{ij} \sin\left(\delta_i - \delta_j\right) - B_{ij} \cos\left(\delta_i - \delta_j\right) \right] V_j, \quad \forall i \in N \tag{3-6}$$

From the power flow equations (3-5) and (3-6), it is clear that the OPF is a nonlinear optimization problem. The active and reactive powers on each bus are affected by both magnitude and phase angle of the bus voltage. In order to simplify the problem, decoupled power flow equations [63] are used in OPF by utilizing the weak coupling of the bus voltage magnitude and phase angle in the transmission grid [81], [82], and the OPF problem is therefore decomposed into two subproblems, P-problem and Q-problem. By assuming constant magnitudes of bus voltages, the active power is only affected by the phase angle of bus voltages. Therefore, the P-problem is the minimization of generation cost by adjusting the active power output from generators. The Q-problem is to minimize the active power transmission losses by assuming the constant phase angles of bus voltages. The P-problem can be further approximated to a dc OPF because the active power is linearly related to the phase angles of bus voltages, just like the relationship between power and bus voltage in a dc grid [83], [84]. Correspondingly, the OPF using complete power flow equations is called ac OPF.

3.1.2 Solution Methods

The electric power system is, generally, large and complex, and could include thousands of buses, various types of devices, and strict constraints. Therefore, the optimal power flow is a very large and difficult mathematical programming problem. Several mathematical approaches have been considered to develop reliable solution to the OPF problem reliably. The detailed presentation of these approaches can be found in [85]-[87]. A short introduction of some solution methods is given below.

- Linear based Programming (LP)

The LP formulation requires linearization of the objective function and constraints with nonnegative variables, and then the simplex method is applied to solve the OPF problem [88]. LP or LP based methods are commonly used in solving the OPF problem.

- Mixed Integer Programming (MIP)

MIP aims at solving the OPF problem with constraints involving integer variables

[89]. It is developed on the basis of LP, and is employed to solve typical OPF problems with discrete variables, such as tap changer positions, breaker statues, etc.

- Non-Linear Programming (NLP)

NLP deals with problems with nonlinear objective and constraint functions. The ac OPF is a typical nonlinear problem because of the nonlinearity of the power flow equations. NLP has two types, constraint NLP and unconstraint NLP. The constraint NLP can be transferred to unconstraint NLP using Lagrangian or penalty function methods. Many algebraic programming methods can be employed for the unconstraint NLP. A simplified gradient descent algorithm is firstly presented in [64] in solving NLP. The further development of NLP can be found in [90]-[92].

- Quadratic Programming (QP)

QP is a special form of NLP which is proposed firstly in [93]. It solves the OPF problem with the quadratic objective function and linear constraints. Further improvements of this method can be found in [94], [95].

- Interior Point method (IP)

IP handles both linear and nonlinear optimization problems, whose basic idea is to search for an optimal point in a feasible region [96]. Some improved IP method are proposed, such as the Predictor Corrector Primal Dual Interior Point Method (PCPDIPM) for solving the optimal reactive power flow [97], and the Step-Controlled primal-dual Interior Point Method (SCIPM) to enhance the convergence of market-based OPF computation [98].

Besides the classical optimization methods introduced in the above, some Artificial Intelligence (AI) methods are also employed in solving the OPF problem in order to get better optimal solutions and lower the sensitivity to initial conditions. These AI methods include Genetic Algorithm method (GA) [99], Evolutionary Programming (EP) [100], Particle Swarm Optimization (PSO) [101], etc.

Optimization software and solvers which can be used in the modeling and solving the OPF problem can be found as both commercial version or free version. For example, General Algebraic Modeling System (GAMS) is a general mathematic modeling software, which is designed for modeling linear, nonlinear and mixed integer optimization problems [102]. The defined OPF model in GAMS is solved by calling solvers. Some electric power system analysis software also supply OPF package to solve OPF problems, such as MatPower, PSS/E, etc.

3.2 Transmission Expansion Planning Methods

3.2.1 State of the art

The transmission expansion planning is characterized by its complex and multi-object feature. The development of the electric power market and the renewable power generation within decades make it even more complex.

Before the deregulation, the electric power system was vertically integrated. The generation, transmission, and distribution parts are centrally managed by one operator. The decision on expansion projects was based on the both generation and transmission cost minimization principle [103] with the satisfaction of the system steady-state and dynamic technical constraints to make sure the adequate and reliable power supply and the system economic operation. In the deregulated electricity market, which started around the end of the 90th, the generation, transmission, and distribution systems are separated as independently managed parts from one complete power system. The Transmission System Operators (TSOs) are only responsible to the transmission system in some countries. Meanwhile, the electricity power market appears and has shown its power in the development of the electric power system. Therefore, the expansion of the transmission system is driven by market based initiatives, and the objects focus on the maximum social welfare by increasing transmission capacity to allow the most efficient use of generation, and the maximum system reliability and security of power supply and fostering market [66].

The whole process of the transmission expansion planning usually includes the following steps [66] as shown in Figure 3.1. In the first step, the scenarios are prepared by forecasting the changes of the load demand, power exchange between countries during the planning horizon, and other factors, e.g., the economic, policy, public options, etc. The system simulation and studies to check the security and adequacy of the system operation and power supplying in both steady and dynamic states are carried out in the second step on the basis of the prepared scenarios. The studies generally take into account the N-1 criterion or even N-2 criterion in specific cases to check if there are any violations of the operation limits, e.g., bus voltage limits, transmission capacity limits, etc., during contingencies. The results of the system studies will address the specific problems of the existing system, and suggest the preliminary expansion requirements and solutions for the problems using different methods or technologies. Then, the cost benefit analysis approach will be used to evaluate the techno-economic indices of all suggested expansion solutions. The preferred expansion solutions will be identified by ranking all suggested solutions based on both the techno-economic indices and the environmental assessment results. Finally, the expansion decisions will be made on the basis of all the above analysis results.

After the deregulation of the electric power system, numerous studies focusing on the various aspects of the transmission expansion planning in a competitive

electricity market were proposed [66], [104], and [105], e.g., simulating the electricity market, modeling the electric power system, defining the objective functions, etc. The transmission expansion planning process and methodologies commonly used nowadays in practices is introduced in [66] and [67]. The whole planning process is identified as a multi-objective task with consideration of uncertainties and risk situations, and the cost benefit analysis for the economic assessment of alternatives is generally used during the planning process [66].

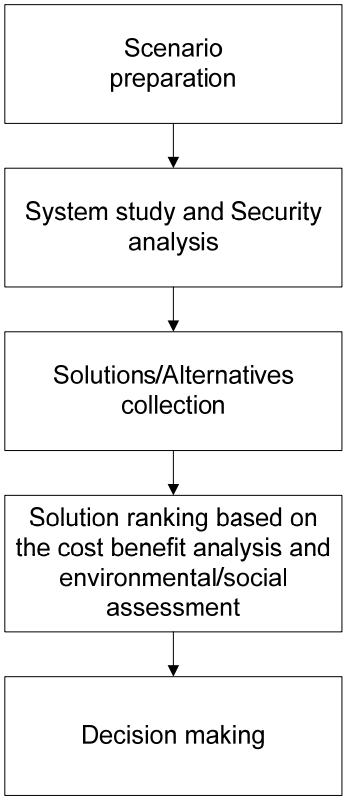

Figure 3.1. Transmission expansion planning process.

3.2.2 Cost-benefit analysis approach

The cost benefit analysis approach was firstly developed from the welfare economics theories to help the investment decision in 1930th [106]. Then it was applied in the electricity investment area to compare the alternatives of hydropower and thermal power plants. Nowadays, it has been widely used as a key method in the transmission expansion planning process to identify the preferred expansion alternatives among all possible solutions as described in Section 3.2.1

The concept of the cost benefit analysis is to have a complete evaluation and understanding of a project's economics and its influence on the existing system or society by comparing all the related costs and potential benefits in monetary terms.

Its results can provide supporting information to decision makers, e.g., if the project can bring a net gain [107]. Therefore, the key part of this approach is the identification of the costs and benefits. In the transmission expansion planning process, the costs of a reinforcement project within the whole project life cycle are suggested to be considered by ENTSO-E [108]. They generally include the material cost, construction cost (e.g., the assembly and dismantling cost, cost for temporary solutions which are necessary to realize a project, etc.), administration cost (cost for approval procedure), and operation cost, etc.

The expected benefits from a transmission expansion project are diverse from TSOs nowadays after the deregulation of the electric power system. As it is mentioned in [66] and [108], they could be the socio-economic welfare (avoided generation cost or increased surplus of all market players), the increased energy efficiency (avoided power losses), reduction in CO_2 emissions, integration of the renewable energy resources, improvement of the power supply, improvement of the system robustness and flexibility, and so on. Two methods can be used to calculate the expected benefits. One is the "Take Out One at the Time (TOOT)" method, another is the "Put IN one at the Time (PINT)" method. The TOOT method is to exclude the expansion alternatives one by one from the forecasted system network and to evaluate the benefits by comparing the results with and without the examined alternatives. In contrast, PINT method is to include the expansion alternatives one by one into the original system network and evaluate the benefits.

Some drawbacks of the cost benefit analysis approach lie in its application of the transmission expansion planning, especially after the deregulation of the power system and the environment issues are more and more concerned by the public. It can be seen from the potential benefits listed above that most of them are conflicting with each other, and some of them are difficult to be monetized. Therefore, some benefits cannot be included in the cost benefit analysis. Meanwhile, one single indicator from the cost benefit analysis cannot comprehensively reflect the effects of one expansion alternative to the power system, power market, and the society. To avoid the drawbacks of the cost benefit analysis approach, an overall assessment method is suggested by ENTSO-E [108], which evaluates the economics of alternatives on the basis of multi-criteria. In [66], one more section, the environmental and social assessment is added after the traditional techno-economic assessment based on the cost benefit analysis to take into account the economical and social issues.

Chapter 4

Proposed Mixed AC/DC Optimal Power Flow

This chapter presents a proposed Mixed ac/dc OPF (M-OPF) on the basis of the traditional ac grid OPF incorporating the developed VSC-MTDC model. This M-OPF model will be used in the evaluation of the benefits from using embedded VSC-MTDC in an ac transmission grid. Before the introduction of the M-OPF model, a steady-state model of VSC-MTDC is developed. The implementation of the M-OPF model in GAMS and MATLAB is shown at the end of this chapter. A six bus network is used for the verification of this M-OPF.

4.1 Modeling of VSC-MTDC

A general mixed ac/dc system with VSC stations is depicted in Figure 4.1. As can be seen, the mixed ac/dc system consists of two major parts: the meshed ac grid and the dc grid which are connected by VSC stations at some buses. The ac network may represent ac buses, transmission lines, transformers, shunt capacitors/reactors, etc. The dc grid includes dc buses, dc cables or overhead lines, etc. The dc loads and dc/dc converters used to transfer dc voltages to different levels may also be included in the dc network. However, they are not considered in this thesis. The configuration of the VSC station shown in Figure 4.1 refers to the traditional two- or three-level converter. When MMC with the cascade connection modulation method is used, ac filters can be omitted [32], as described in Section 2.1.

4.1.1 Review of Normal Power Flow Calculation of the Mixed ac/dc grid

The conventional ac power flow calculation method uses active and reactive power injections from generators as known quantities to calculate variables, e.g., bus voltages and angles. When the VSC station is connected to an ac bus via a transformer, its active and reactive power outputs are usually controlled at the PCC bus by operators as described in Section 2.3.3. Therefore, they are also considered as known quantities in the power flow equations. The same concept is

applied to the power flow calculation of a meshed dc grid. The dc power injection from VSC, (i.e., P_{cdc} as shown in Figure 4.1), is used as a known quantity to calculate the dc bus voltages. If the VSC is treated as a lossless power exchanger, the dc power injection (P_{cdc}) will have the same magnitude but opposite direction of the ac power injection (P_c). Therefore, the key point of solving the power flow equations of the dc grid is to find the ac power injection (P_c) from the ac side. However, the power at the PCC bus (P_{pcc} and Q_{pcc}) are known, while the power at the VSC ac terminal (P_c and Q_c) are unknown in the power flow calculation. Therefore, in order to solve the power flow equations of a meshed dc grid, the ac power (P_c) has to be first calculated on the basis of the controlled ac power at PCC bus (P_{pcc} and Q_{pcc}) and the initial bus voltages or the bus voltages from the previous step of the iterative loop when the Newton-Raphson method is used as described in [55]. This calculation step would increase the complexity of computation burden when included in the OPF model and might lead to difficulties in obtaining the solutions from the OPF model.

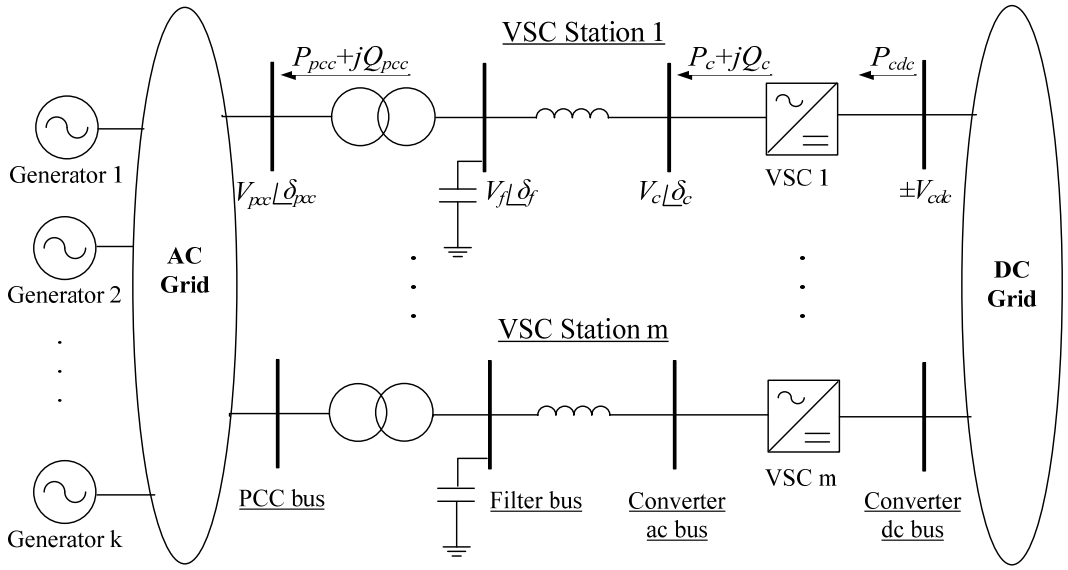

Figure 4.1. The ac grid with an embedded VSC-MTDC system.

4.1.2 Proposed Approach for Incorporating the VSC-MTDC in the M-OPF Model

As described in Section 3.1.1, the controlled power injections from generators and VSC stations to the ac or dc grids are considered as the decision variables in an OPF model. When a certain power flow solution is settled and if the transformer ratio is fixed, the optimal solution at the PCC bus (i.e., P_{pcc}, Q_{pcc}, V_{pcc}, and δ_{pcc}) will have only one corresponding optimal solution on the converter ac bus (i.e., P_c, Q_c, V_c, and δ_c). Therefore, the active and reactive powers flowing from the VSC to the converter ac bus (P_c and Q_c) can be used as the decision variables in the M-OPF model, instead of the active and reactive power injections at the PCC bus (P_{pcc} and Q_{pcc}). This yields the fact that pre-calculating the power flow from the

PCC bus to the converter ac bus would be unnecessary, which would simplify calculations and reduce computation time.

Thus, the proposed basic approach is described in the following:

- VSCs function as power sources injecting ac and dc power into two sides separately. If the power losses of the VSC were neglected, the injected ac and dc active power from VSCs have the same magnitudes but with opposite directions.

- The injected power from VSCs to the ac and dc grids are limited by the adopted constraints from both the ac and dc sides, including maximum bus voltage limits, maximum valve current limit, etc.

- The power flow equations of the ac and dc grids are coupled by the active power exchange through VSCs. They can be used directly and solved simultaneously in the M-OPF model.

4.2 Mathematic Model of the VSC Station

The VSC station is modeled in steady state according to the proposed approach described above. The VSC station model includes two parts: 1) the power and voltage relationships between ac and dc sides; 2) VSC capacity constraints.

4.2.1 Power and Voltage Relationships between ac and dc Grids

As discussed above, the VSC is considered as an electric power exchanger. When power losses are neglected, the power exchange of the VSC is defined in (4-1),

$$P_c = -P_{cdc} \tag{4-1}$$

In order to avoid the harmonics because of the over-modulation of the VSC, the peak value of the phase voltage at the converter ac bus is assumed to be lower than the corresponding converter dc bus voltage in this thesis as suggested in [33]. Thus, the voltage relationship between ac and dc bus of the VSC can be given by (4-2):

$$\bar{V}_c = \left(\sqrt{3}/\sqrt{2}\right) V_{cdc} \tag{4-2}$$

If the nominal dc and ac voltages are both set at 1 p.u., equation (4-2) can be re-written in the per unit form as expressed in (4-3), where the voltage relationship factor (k_v) is defined by the allowed maximum ac bus voltage.

$$\bar{V}_c = k_v V_{cdc} \tag{4-3}$$

If the maximum ac voltage generated by VSC is not same as the allowed maximum ac bus voltage for insulation purpose, the voltage relationship factor (k_v) can be modified based on the lower limit of these two constraints. The voltage at the VSC ac bus is limited by (4-4).

$$V_c \le \bar{V}_c \tag{4-4}$$

4.2.2 VSC Capacity Constraints

The basic constraints of a VSC station have been discussed in Section 2.3.3, i.e., the maximum current through VSC valves and the maximum dc voltage. The former determines the maximum VSC apparent power limit, and the latter defines the VSC reactive power output limit. Usually, VSC constraints are applied at the PCC bus as described above. In this OPF model, the VSC constraints at the converter ac bus are used because the VSC power exchange at the converter ac bus is set as decision variables.

- Maximum Apparent Power Constraint

Given the maximum valve current, the apparent power of VSC is given by (4-5):

$$\left|S_c\right| \le \left|V_c \bar{I}_v\right| \tag{4-5}$$

Equation (4-5) can be re-written as in (4-6):

$$\sqrt{P_c^{\,2} + Q_c^{\,2}} \le \left|V_c \bar{I}_v\right| \tag{4-6}$$

The apparent power range on the VSC power plane defined by (4-6) can be plotted as shown in Figure 4.2.

- Maximum Reactive Power Constraint

The maximum reactive power constraint of the VSC is defined in (4-7), assuming that the conductance of the phase reactor is much smaller than its susceptance.

$$\bar{Q}_c = -B_r \left(\bar{V}_c^2 - \bar{V}_c V_f e^{j\left(\delta_c - \delta_f\right)} \right) \tag{4-7}$$

As can be seen in Figure 4.2, the reactive power variation (the dotted red curve) inside the circle is quite small compared to the nominal VSC rating (about 3% of the nominal VSC rating in this case). To simplify the calculation, the maximum reactive power output limit is set as a constant limit, the minimum value of the calculated maximum reactive power limits when δ_c - δ_f = 0. The maximum reactive power constraint of the VSC can be simplified as in (4-8).

$$\overline{Q}_c = -B_r\left(\overline{V}_c^2 - \overline{V}_c V_f\right) \tag{4-8}$$

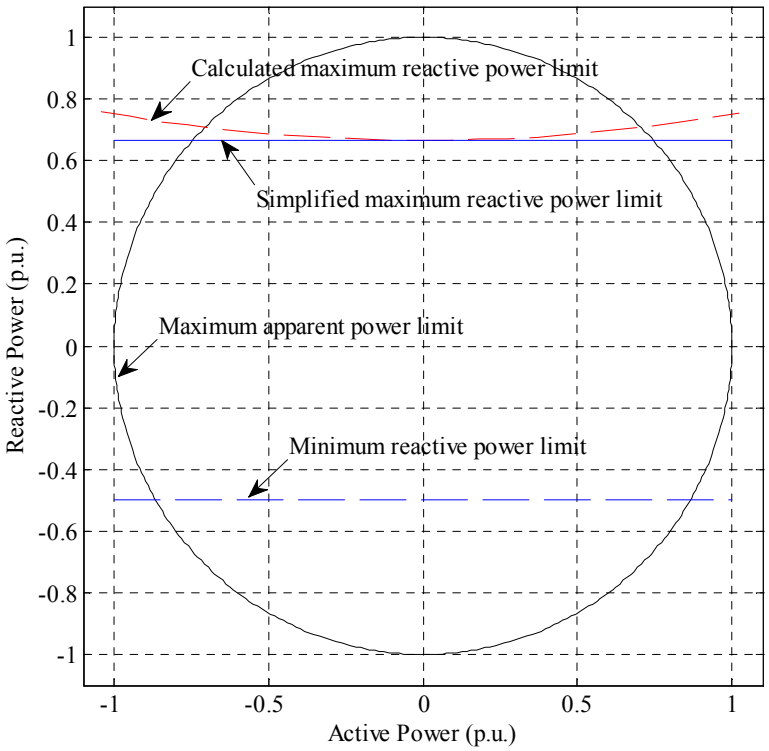

Figure 4.2. Example of the VSC power capacity curves with the assumed parameters: $\overline{I}_v$ = 1 p.u., Vc = 1 p.u., Vf = 0.9 p.u., Rr = 0.0001 p.u., and Xr = 0.15 p.u..

- Minimum Reactive Power Constraint

The minimum reactive power constraint of the VSC is expressed by (4-9). This limit depends on the specific requirement of each project. In this study, it is assumed as a fixed value in order to simplify the model, as shown in Figure 4.2. The constraint factor (k_Q) is, normally, decided by the design of the real project.

$$\underline{Q}_c = -k_Q S_{nom} \tag{4-9}$$

4.3 The Proposed M-OPF model

This section presents the objective functions and constraints of the proposed mixed ac/dc OPF model referred to as M-OPF. It shall be clarified that the variables used in the equations of Section 4.2 will be specified with indices in this Section. For example, P_c in (4-1) will be presented as P_{ci} in (4-16), which indicates the power injection to the bus i.

4.3.1 Objective Functions

- Minimization of Total Generating Cost

The first objective function considered in the M-OPF model is the minimization of the total generation cost as given by (4-10):

$$\text{Minimize} \quad Cost = \sum_{i=1}^{NG} (A_{ci} + B_{ci} P_{gi} + C_{ci} P_{gi}^2) \tag{4-10}$$

- Minimization of Total Transmission Loss

The second objective function considered in the M-OPF model is the minimization of the total active power loss of the mixed ac/dc system as given by (4-11):

$$\text{Minimize} \quad P_{loss} = P_{acloss} + P_{dcloss} + P_{vscloss} \tag{4-11}$$

The total active power loss includes three components: 1) active power loss of the ac transmission lines; 2) active power loss on dc underground cables; and 3) active power losses of VSCs described in the following:

1) Active power loss of the ac transmission lines can be calculated using (4-12) [109]:

$$P_{acloss} = 0.5 \sum_{i=1}^{N} \sum_{j=1}^{N} g_{ij} \left(V_i^2 + V_j^2 - 2 V_i V_j \cos\left(\delta_i - \delta_j\right) \right) \tag{4-12}$$

2) Active power loss on dc underground cables can be calculated using (4-13):

$$P_{dcloss} = \sum_{i_{dc}=1}^{M} \sum_{j_{dc}=1}^{M} g_{i_{dc} j_{dc}} \left(V_{i_{dc}} - V_{j_{dc}} \right)^2 \tag{4-13}$$

3) Active power loss of VSCs can be expressed as a quadratic function of the phase current of VSC valves as shown in (4-14) [110]:

$$P_{vscloss} = \sum_{i=1}^{M} (A_{li} + B_{li} I_{vi} + C_{li} I_{vi}^2) \tag{4-14}$$

,where the phase current of VSC valves can be calculated using (4-15):

$$\left(I_{vi} V_{ci} \right)^2 = {P_{ci}}^2 + {Q_{ci}}^2 \quad \forall i \in M \tag{4-15}$$

4.3.2 Constraints

The two objective functions described above are subjected separately to the same

set of technical constraints.

4.3.2.1 Constraints from the ac System [63]:

- AC load flow equations:

The load flow equations of the ac grid are modified by incorporating the active power injections from VSCs and the VSC losses as shown in (4-16) and (4-17):

$$P_{gi} + P_{ci} - P_{di} - P_{vsclossi} = V_i \sum_{j=1}^{N} \left(G_{ij} \cos\left(\delta_i - \delta_j\right) + B_{ij} \sin\left(\delta_i - \delta_j\right)\right) V_j \quad \forall i \in N \tag{4-16}$$

$$Q_{gi} + Q_{ci} - Q_{di} = V_i \sum_{j=1}^{N} \left[G_{ij} \sin\left(\delta_i - \delta_j\right) - B_{ij} \cos\left(\delta_i - \delta_j\right)\right] V_j \quad \forall i \in N \tag{4-17}$$

- Generator active and reactive power limits:

$$\underline{\mathrm{P}}_{gi} \le \mathrm{P}_{gi} \le \overline{\mathrm{P}}_{gi} \quad \forall i \in NG \tag{4-18}$$

$$\underline{\mathrm{Q}}_{gi} \le \mathrm{Q}_{gi} \le \overline{\mathrm{Q}}_{gi} \quad \forall i \in NG \tag{4-19}$$

- AC bus voltage limits:

$$\underline{V}_i \le V_i \le \overline{V}_i \quad \forall i \in N \tag{4-20}$$

- AC transmission line capacity limit:

$$\underline{S}_{ij} \le S_{ij} \le \overline{S}_{ij} \quad \forall i \in N, \ \forall j \in N \tag{4-21}$$

4.3.2.2 Constraints from the VSC-MTDC System [55], [111]:

- The dc load flow equations:

The balanced bipolar VSC configuration is considered as the normal operation mode in this study. The dc load flow equations of this configuration may be expressed in the following way (4-22):

$$P_{i_{dc}} = 2V_{i_{dc}} \sum_{j_{dc}=1}^{M} G_{i_{dc}j_{dc}} V_{j_{dc}} \quad \forall i_{dc} \in M \tag{4-22}$$

- The dc bus voltage limits:

$$\underline{V}_{i_{dc}} \le V_{i_{dc}} \le \overline{V}_{i_{dc}} \quad \forall i_{dc} \in M \tag{4-23}$$

- The dc transmission line flow limits:

$$\underline{P}_{i_{dc}j_{dc}} \le P_{i_{dc}j_{dc}} \le \overline{P}_{i_{dc}j_{dc}} \quad \forall i_{dc} \in M, \quad \forall j_{dc} \in M \tag{4-24}$$

4.3.2.3 The Constraints on VSC:

Specific constraints of the VSC model have been previously introduced in Section 4.2. The equations (4-1), (4-3), (4-4), (4-6), (4-8), and (4-9) are included in the M-OPF model.

4.4 Implementation of M-OPF in GAMS and MATLAB

The proposed M-OPF model is implemented using the General Algebraic Modeling System (GAMS) [102] and solved with the nonlinear solver Interior Point Optimizer (IPOPT) [112]. MATLAB is employed in data preparation and results processing. The structure of the calculation process and the program code is shown in Figure 4.3. The data of the electric power system are stored in a general form in Excel sheets, including network parameters, generator capacity limits, VSC-MTDC parameters, etc. MATLAB reads data from Excel sheets, converts them into the format specified by GAMS, and then sends the data to GAMS. The M-OPF model is built in GAMS including the objective functions and all constraints. GAMS is also used to calculate the Y matrix and define decision variables. By calling solvers, the M-OPF model is solved and results are obtained. The results of the M-OPF are read from GAMS by MATLAB again, converted to readable result data, and then written into Excel sheets.

It should be noted that the non-linear optimization problem could yield local optimum solutions. In order to get better optimum solutions, some popularly used solvers, including MINOS, CONOPT, and IPOPT, were tested in solving the M-OPF model, which will be shown in Section 4.5.3. From the test results, the IPOPT solver was proofed to be the best one in solving M-OPF model because it gives the best results comparing to the results obtained from other solvers. It uses an "interior point line search filter" method [112], and is a commonly used in solving large-scale nonlinear optimization problems. The default value of the relative convergence tolerance of the algorithm of IPOPT is 10^{-8}.

On the other hand, the focus in this thesis is on the formulation of the M-OPF model rather than on the development of the advanced solution algorithms for the global optimum of the non-linear optimization problem. For different (local optimal) solutions with the same objective function value, the total benefits obtained based on local optimums could be the same, however, the generation dispatches and system losses could be different. The focus of the analysis in this

thesis is on the total benefits to evaluate the economics of VSC-MTDC alternatives which is therefore not affected by this issue.

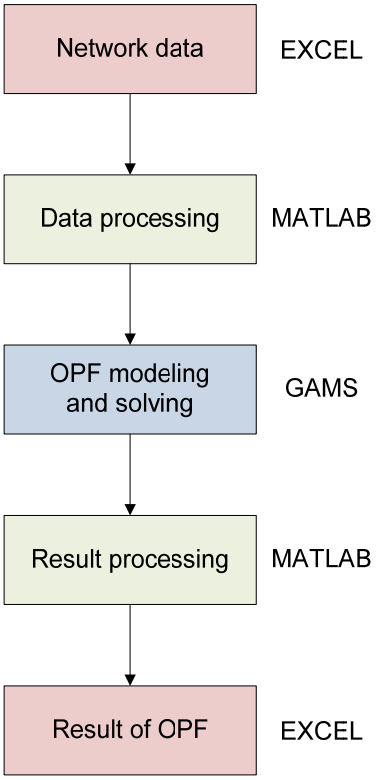

Figure 4.3. The flow chart of the implemented OPF solving process.

4.5 Verification using a six-bus network

In this thesis, the M-OPF model is verified by comparing its OPF results with the results from PowerWorld [113] using a modified 6-bus network with an embedded VSC-MTDC system.

4.5.1 Description of 6-bus Network

The 6-bus system used in the verification of the M-OPF model is described in [109]. The system includes two generators, six loads, and two shunt capacitors. Figure 4.4 shows the network configuration of this system. The network parameters are listed in Appendix B. (Table B-1 and Table B-2).

In order to embed a VSC-MTDC system, three ac transmission lines are replaced with three dc links. Thus, a mixed ac/dc system based on VSC is obtained. Figure 4.5 shows the modified network, in which the three-terminal VSC-MTDC system is included and marked by the red color. Three dc busses are added to the network. DC buses are named after the corresponding ac buses. Inside each VSC station, two more ac busses are added, the VSC ac terminal bus and the ac filter buss, as illustrated in Figure 4.1. Three VSC stations are assumed having identical

configuration and identical parameters. The parameters of VSC station are listed in Table 4.1.

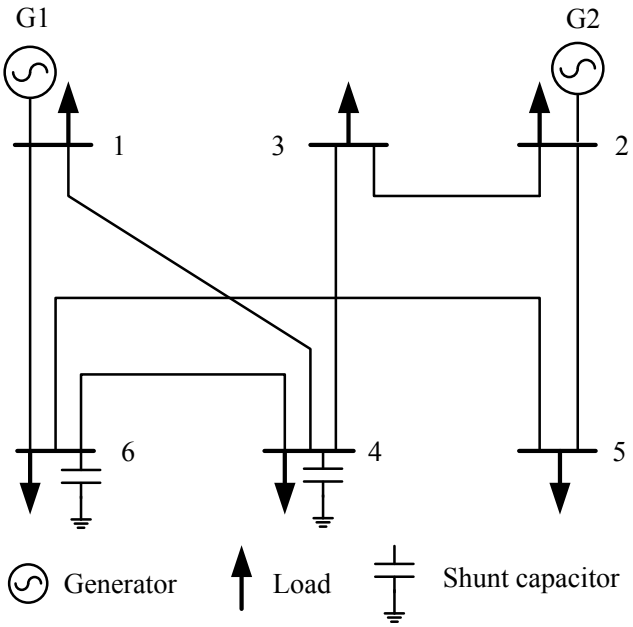

Figure 4.4. Network of six-bus system.

4.5.2 Verification Method

The M-OPF model presented in Section 3 incorporates the VSC station model with a detailed configuration, and the dynamic constraints are applied in the model, e.g., the VSC ac terminal voltage is limited by VSC dc terminal voltage. Therefore, there is not commercial software which can be utilized to accurately verify the results of the M-OPF model. An approximate verification is done in this study to check the correction of power flow results from M-OPF. The mixed ac/dc network shown in Figure 4.5 is further simplified by replacing the VSC stations with corresponding loads, and removing the dc cables. Therefore, the mixed ac/dc network is simplified to an ac network, which can be implemented in commercial power system analysis software, e.g., PowerWorld [113]. The power flow results of the M-OPF model is approximately verified by comparing them to the results from this simplified network simulated in PowerWorld. In order to reduce the impact from the losses of dc cables to the power flow results in the M-OPF model, the values of dc cable resistance are set to a small value, 0.001 p.u.. Figure 4.6 shows the simplified network in PowerWorld. Six loads corresponding to exchanged power and losses of three VSC stations are marked by blue and green frames.

The results from both M-OPF model and simplified network implemented in PowerWorld are shown in tables, from Table 4.2 to Table 4.5. It can be seen that the results from two cases, e.g., bus voltages, generator power outputs, and the

power flow on ac lines, are almost same. Therefore, the power flow results of M-OPF model implemented in GAMS is proofed to be correct. It should be noted that this verification method can only verify the correction of the power flow from M-OPF, while the optimum of the power flow from M-OPF cannot be proofed.

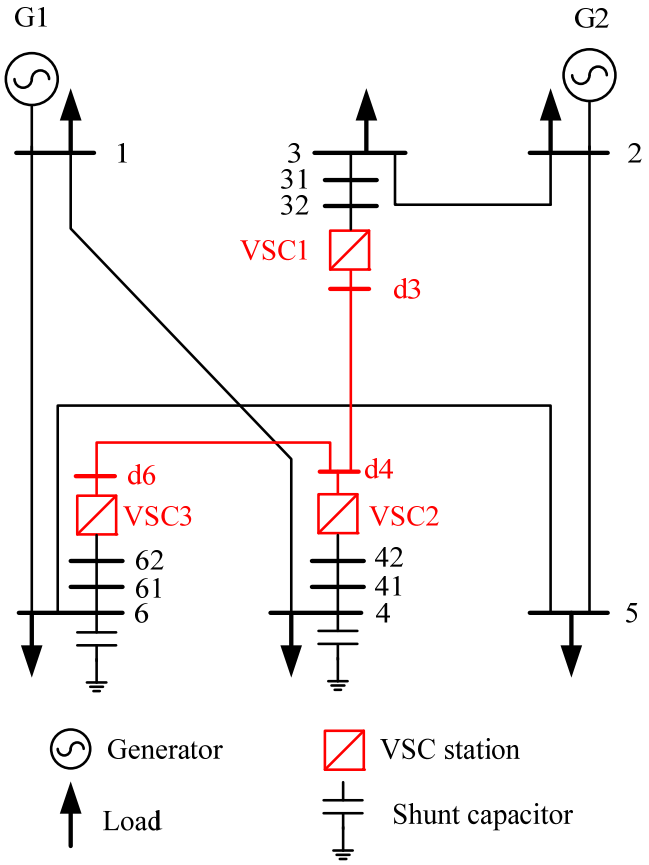

Figure 4.5. Mixed ac/dc system with a three-terminal VSC-MTDC system.

Table 4.1. VSC station parameters

VSC station parameters					
S_{nom}	1 p.u.	X_r	0.15 p.u.	A_l	0.011
S_{base}	100 MVA	R_r	0.0001 p.u.	B_l	0.0029
V_{dcnom}	± 1 p.u.	B_f	0.15 p.u.	C_l	0.0037
$\overline{I_v}$	1 p.u.	X_{tr}	0.1 p.u.		
		R_{tr}	0.0001 p.u.		

4.5.3 Performance Test of Different Solvers in Solving M-OPF model

As discussed in Section 4.4, the proposed M-OPF model is a non-linear optimization problem, which could yield local optimum solutions. In order to test the performance of nonlinear solvers in solving this M-OPF model, different popularly used solvers including MINOS, CONOPT, and IPOPT, are tried to solve the M-OPF model in this study. For this six-bus system, the IPOPT solver

gives the best results compared to the results obtained from other solvers. The comparison of the results from these three solvers is show in Table 4.6.

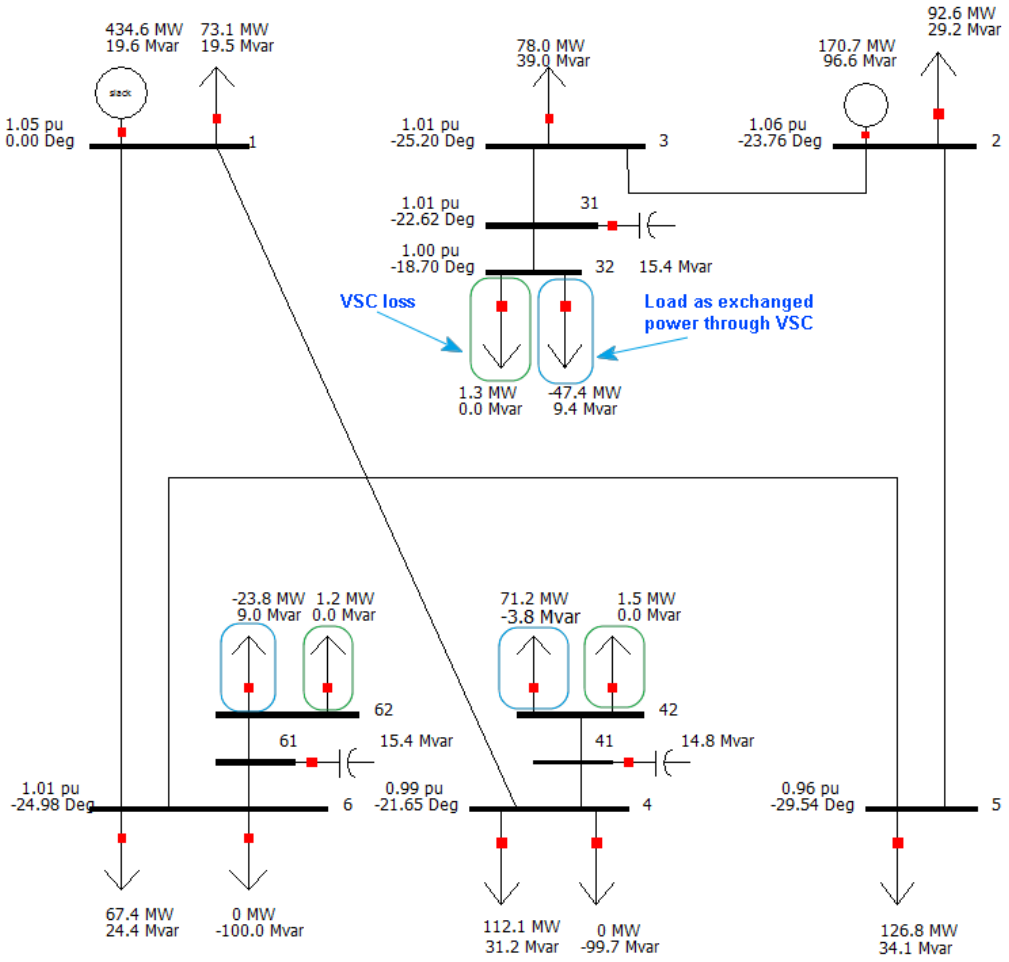

Figure 4.6. Simplified mixed ac/dc network in PowerWorld.

Table 4.2. Comparison of bus voltage from M-OPF model and PowerWorld

Bus Voltage				
Bus Num	Voltage Magnitude (p.u.)		Angle (degree)	
	GAMS	PowerWorld	GAMS	PowerWorld
1	1.050	1.050	0	0
2	1.060	1.060	-23.72	-23.76
3	1.000	1.012	-25.17	-25.20
4	0.987	0.987	-21.66	-21.65
5	0.961	0.960	-29.52	-29.54
6	1.008	1.007	-24.97	-24.98

Table 4.3. Comparison of power generation from M-OPF model and PowerWorld

Power Generation				
Generator	Active Power (MW)		Reactive Power (Mvar)	
	GAMS	PowerWorld	GAMS	PowerWorld
G1	434.8	434.6	18.6	19.61
G2	170.7	170.7	95.3	96.59

Table 4.4. Comparison of power flow from M-OPF model and PowerWorld

Power Flow				
Transmission Line	Active Power Flow (MW)		Reactive Power Flow (Mvar)	
	GAMS	PowerWorld	GAMS	PowerWorld
1-4	211.9	211.7	-0.8	-0.6
1-6	149.8	149.8	0.5	0.7
2-3	32.4	32.4	40.1	40.6
2-5	45.6	45.7	26.0	26.7
6-5	85.8	85.8	20.9	21.0

Table 4.5. Exchanged power from ac to dc side

Exchanged Power from ac to dc side			
VSC	Active Power (MW)	Reactive Power (Mvar)	VSC Power Loss (MW)
VSC 1	-47.4	9.4	1.3
VSC 2	71.2	-3.8	1.5
VSC 3	-23.8	9.0	1.2

Table 4.6. Comparison of optimal results using three different solvers

Solver	Minimization of Generation Cost	Minimization of System Power Losses
IPOPT	2.9614+E5	0.2570
MINOS	3.1976+E5	0.2705
CONOPT	3.2113+E5	Infeasible Solution

Chapter 5

Generation Cost Reduction and Power Loss Reduction by VSC-MTDC

This chapter analyzes the impact on the generation cost and the system power losses as a result of embedding VSC-MTDC systems into an ac grid. Case studies on the basis of the Nordic 32-bus system using the M-OPF proposed in Chapter 4 are carried out. The case study results are presented, and the main reasons leading to the reduction of the generation cost and the system power loss are analyzed.

5.1 Nordic 32-bus system and case design

5.1.1 Nordic 32-bus System and Assumptions

The Nordic 32-bus system is a benchmark grid representing the fundamental features of the Swedish high voltage transmission system [114]. The single line diagram of the system is shown in Figure 5.1. As can be seen, the system consists of four major areas. The "North" part is the main generation area which is dominated by hydro power plants. More than 50% load demand of the whole system is located in the "Central" area, while the generation capacity in this area is very limited. Thus, the system is characterized by bulk power transmission from north to south through two long transmission corridors, which results in high transmission losses. Meanwhile, the long transmission lines from the "North" to the "Central" area are subject to the voltage instability if the reactive power support is not adequate along the transmission line or at the load area. The "Southwest" area is loosely connected to the "Central" area through two transmission lines, and the "External" area with two busses presents an adjacent network connected to this system. Figure 5.2 shows the distribution of loads and generation capacities in four areas.

Nordic 32-bus system is developed for the study of transient stability and system long-term dynamics. The network data and dynamic models of generators for

dynamic analysis are provided. However, system data for the economic analysis are not included, e.g., the generation cost coefficients. In this study, all generators are classified into four types: hydro plants, nuclear plants, coal thermal plants, and other thermal plants. The cost coefficients for each type of generation are estimated by using the typical values provided in [115]. The values calculated are calibrated using the generation costs of different types in the Nordic countries for 2003 [116]. Finally, they are further adjusted so that the calculated unconstrained market price would be in the current market price range for the Nordic day-ahead market [117]. The calculated cost coefficients for all system generators are provided in Table 5.1.

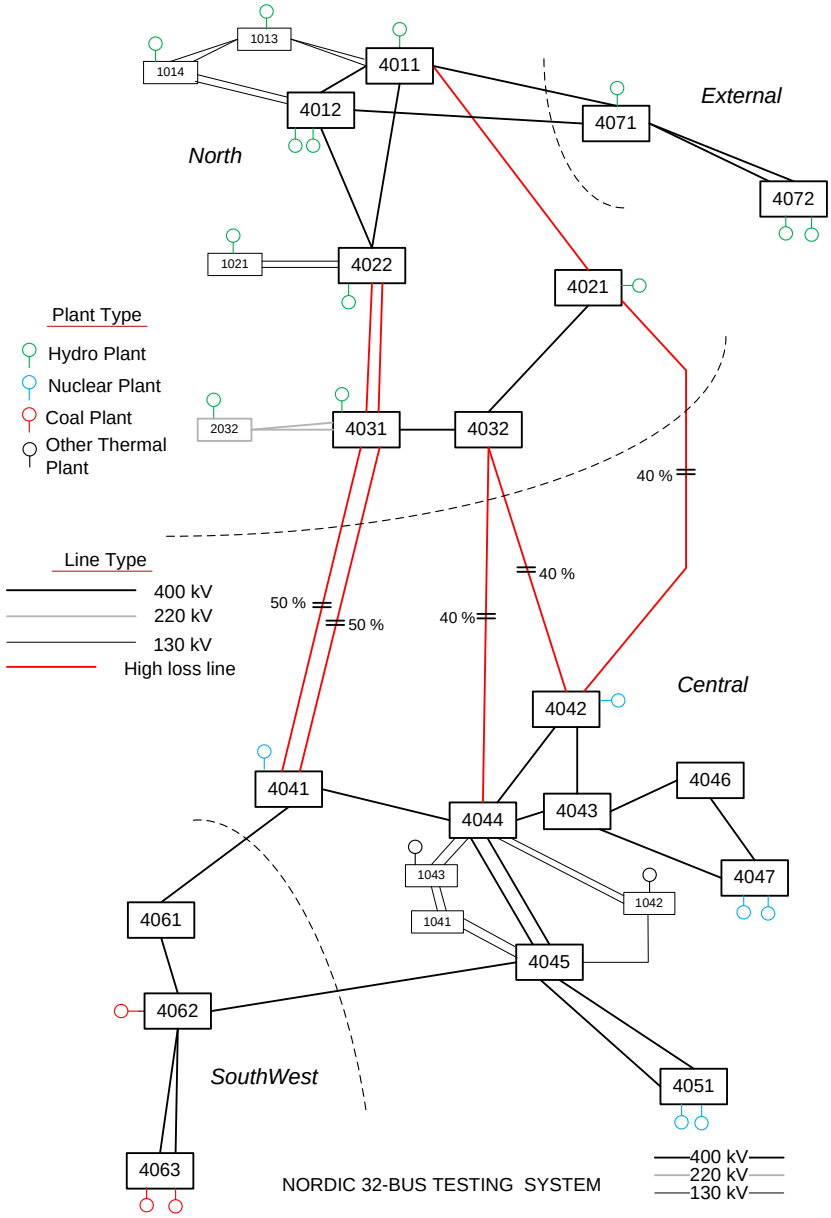

Figure 5.1. Network topology of Nordic 32-bus system.

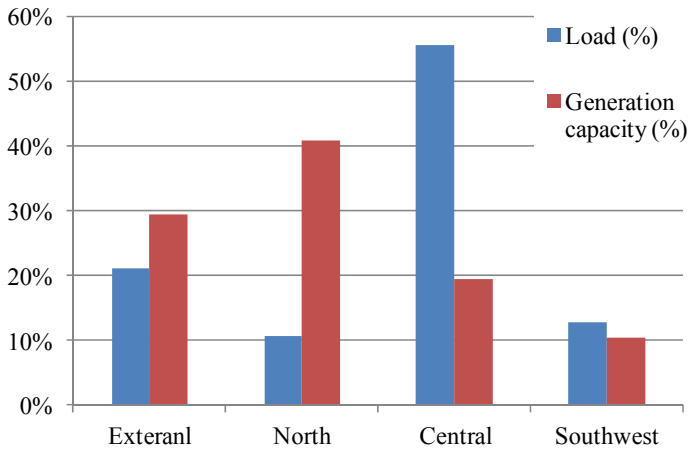

Figure 5.2. Loads and generation capacities of four areas of Nordic 32-bus system.

Table 5.1. Calculated Generator Coat Coefficients

Bus	Ac ($)	Bc ($/MWh)	Cc ($/MW^{2}h)	Plant Type
1012	809	15.4	0.0026	Hydro
1013	1079	20.5	0.0026	Hydro
1014	925	17.6	0.0026	Hydro
1021	1076	20.5	0.0026	Hydro
1022	1619	30.8	0.0026	Hydro
1042	2226	49.2	0.0225	Other thermal
1043	2477	54.8	0.0225	Other thermal
2032	809	15.4	0.0026	Hydro
4011	647	12.3	0.0026	Hydro
4012	809	15.4	0.0026	Hydro
4021	1439	24.7	0.0026	Hydro
4031	1349	25.7	0.0026	Hydro
4042	2070	40.9	0.0048	Nuclear
4047	2229	44.0	0.0048	Nuclear
4047	2229	44.0	0.0048	Nuclear
4051	2070	40.9	0.0048	Nuclear
4051	2070	40.9	0.0048	Nuclear
4062	3264	72.2	0.0297	Coal
4063	3264	72.2	0.0297	Coal
4063	3264	72.2	0.0297	Coal
4071	1076	20.5	0.0026	Hydro
4072	809	15.4	0.0026	Hydro

5.1.2 Definition of the Study Cases

A total of 19 study cases corresponding to the Base Case (i.e., the original Nordic 32-bus system) and other 18 cases representing cases with different VSC-MTDC configurations were considered in this study. The dc cables of the VSC-MTDC system are used to replace corresponding ac transmission lines in each case. The motivation behind the definition of these cases is to increase transmission system

capability, or replace the high loss ac transmission lines by dc underground cables. With the VSC-MTDC system embedded, the transmission system is expected to transfer more hydro power from the North to the South in the system and/or some heavily loaded ac transmission lines could be relieved. Thus, the total generation cost or system power losses could be reduced.

It shall be noted that this study does not focus on the conversion from ac transmission lines to dc cables. The purpose of considering dc cables to replace ac transmission lines in case study is to have a base case, which is the original Nordic 32-bus network. The other cases with VSC-MTDC system can, therefore, be compared with the Base Case. Table 5.2 lists all considered cases.

Table 5.2. VSC-MTDC Systems for Case Study

Case Number	VSC Location (Connected ac bus)	Number of VSC stations	Topology Type
Base Case	Original Nordic 32-bus system		
Case 1	4032 – 4044[(1)]	2	
Case 2	4021 – 4032 – 4044	3	Serial
Case 3	4021 – 4032 – 4031, 4032 – 4044	4	Radial
Case 4	4011 – 4021 – 4032 – 4044	4	Serial
Case 5	4022 – 4031 – 4041	3	Serial
Case 6	4012 – 4022 – 4031 – 4041	4	Serial
Case 7	4022 – 4031 – 4032, 4031 – 4041	4	Radial
Case 8	4011 – 4022 – 4031 – 4041	4	Serial
Case 9	4031 – 4041 – 4044	3	Serial
Case 10	4031 – 4032 – 4044	3	Serial
Case 11	4022 – 4031 – 4032 – 4044	4	Serial
Case 12	4021 – 4032 – 4042 – 4021	3	Ring
Case 13	4032 – 4042 – 4044 – 4032	3	Ring
Case 14	4044 – 4045 – 4051	3	Serial
Case 15	4032 – 4044 – 4045	3	Serial
Case 16	4021 – 4044	2	
Case 17	4011 – 4021 – 4042	3	Serial
Case 18	4011 – 4021 – 4042 – 4044	4	Serial

[(1)] The bus numbers indicate the ac buses which connects the corresponding VSC stations. In addition, one ac transmission line between two buses is replaced by the corresponding dc cable.

It is assumed that the number of terminals of all VSC-MTDC candidates is limited to four and the VSC stations are assumed to be identical. Three types of topology of VSC-MTDC candidates were used: “Serial” type means that all VSC stations are connected by dc cables in series; “Radial” type means that VSC stations are connected by dc cables in a star configuration; “Ring” type means that VSC stations are connected by dc cables in a closed loop. Figure 5.3 shows these topologies.

The converter transformer is assumed to have a fixed turns-ratio. The power loss of a VSC station at the nominal condition is assumed to be 1% of the nominal VSC rating as suggested in [28], referring to the general power loss level of the VSC station using MMC. The effects of the other loss values of a VSC station, i.e., 1.8% for a two-level VSC station and 0.6% for assumed future VSC station loss

level, to the generation cost and the system power loss are also tested by means of sensitivity analyses. The loss coefficients of a VSC station are derived from the "South West Link" HVDC project in Sweden [110], and are scaled to fit the VSC rating used in this study. The main parameters of a VSC station are listed in Table 5.3.

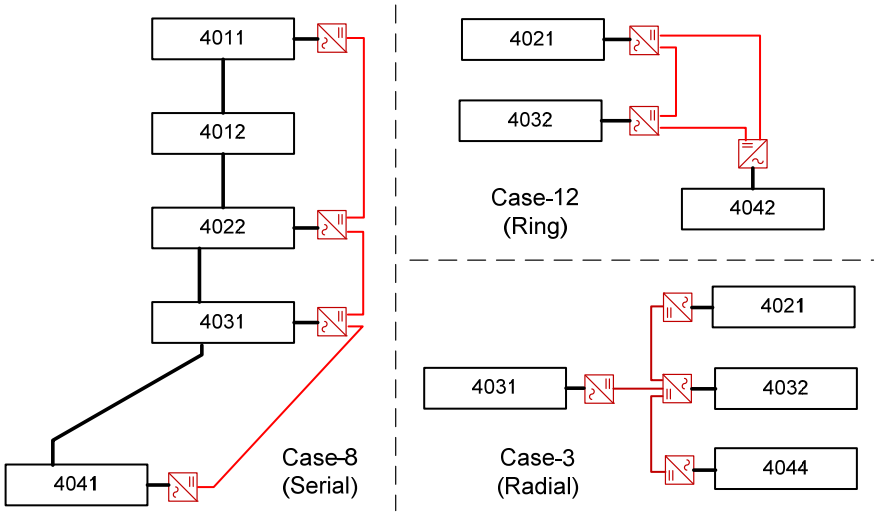

Figure 5.3. Configuration of VSC-MTDC systems of Case-3, Case-8, and Case-12

Table 5.3. Assumed parameters of a VSC station ([7], [110])

VSC station parameters					
S_{nom}	1000 MVA	X_r	0.02 p.u.	R_{tr}	0.0001 p.u.
S_{base}	100 MVA	R_r	0.0001 p.u.	A_l	0.0625
V_{dcnom}	± 300 kV	B_f	2 p.u.	B_l	0.00165
$\overline{I_v}$	10 p.u.	X_{tr}	0.01 p.u.	C_l	0.00021

The type of the dc underground cable is selected from [7] according to the VSC rating. A type of land cable with the aluminum conductor area of 2000 mm^2 is used. In order to obtain the lumped resistance of each dc cable, the length of the corresponding ac transmission line is estimated based on the resistance of the line and the general unit resistance. Thereafter, using the same length of ac transmission line, the lumped resistance of the dc cable can be calculated.

5.2 Generation Cost Reduction Analysis

5.2.1 Results and Discussions

The OPFs with the objective of the generation cost minimization were run for all the 19 cases (including the Base Case) in the nominal load condition. Figure 5.4 shows the results which are normalized with respect to the result of the Base Case. The results are classified by the configuration type of VSC-MTDC systems.

It is clear that the generation costs of modified cases are lower than that of the Base Case in most cases, especially the cases with the "Serial" and "Radial" topology types of VSC-MTDC. Among all cases, Case 8 shows the lowest generation cost, while Case 12 is the worst case. This could be due to the power flow feature of Nordic 32-bus system, and the configurations and locations of VSC-MTDC systems. As discussed in Section 5.1.1, the hydro power generated in the North is cheaper than thermal power generated in the Central and South areas. Meanwhile, the capacity of ac transmission lines connecting the North and Central areas cannot be fully utilized because of the voltage constraint, which limits utilization of the cheap hydro power to decrease the total generation cost. The VSC-MTDC system connecting the North and the Central areas can transfer more hydro power to the load center, and supplies extra reactive power support to the adjacent ac transmission lines to increase their power transmission. Therefore, the generation costs can be reduced by using VSC-MTDC systems in most of cases.

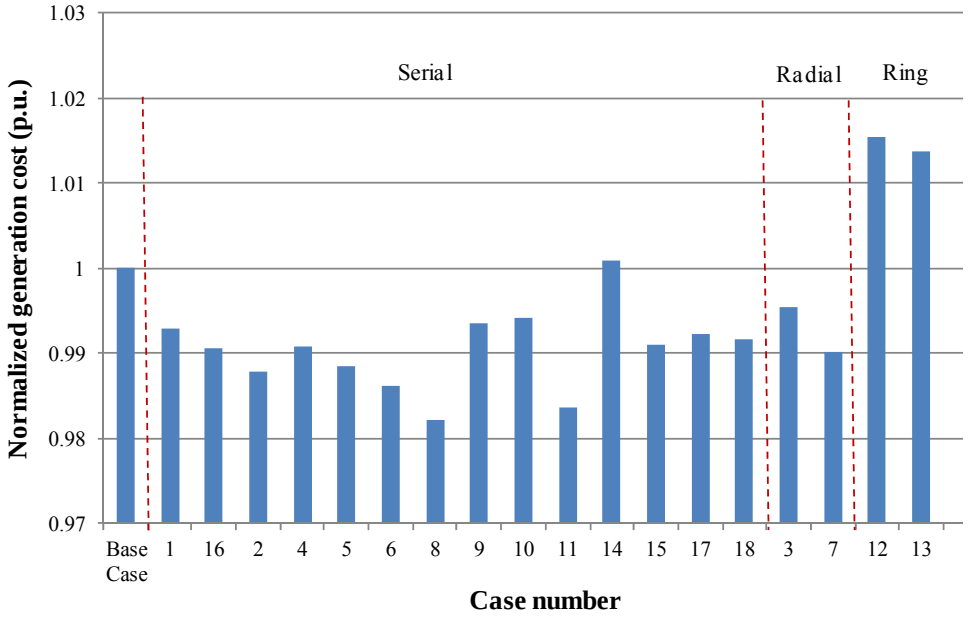

Figure 5.4. Normalized generation costs of 20 cases.

All cases using the "Ring" topology of the VSC-MTDC system show higher generation cost due to the fact that all VSC stations have identical ratings. Two dc cables are connected to one VSC station in the cases using "Ring" topology type, and share the capacity of this VSC station. Therefore, the total capacity of these two dc cables is limited by the capacity of the VSC station, and cannot be fully utilized. Case 14 shows a higher generation cost than that of the Base Case, and also other cases with the same VSC-MTDC system configurations. The reason lies in its location. The whole dc network in Case 14 is located in the Central area, which cannot transfer more low cost hydro power from the North. Meanwhile, the extra power losses introduced by VSC stations aggravate load level in the Central

area. Therefore, The VSC-MTDC system in Case 14 shows opposite influence on the generation cost reduction.

The OPFs with the objective to minimize the total generation cost were also run with different loading levels. The system load was increased equally at all load busses by 0.1 p.u. of each step up to 1.2 p.u.. Figure 5.5 shows the results of the generation cost of selected case in different load conditions. The values of generation costs are normalized with respect to the corresponding result of base case (pure ac grid) in the same load condition, thus, the generation costs of the Base Case are always one for all load conditions.

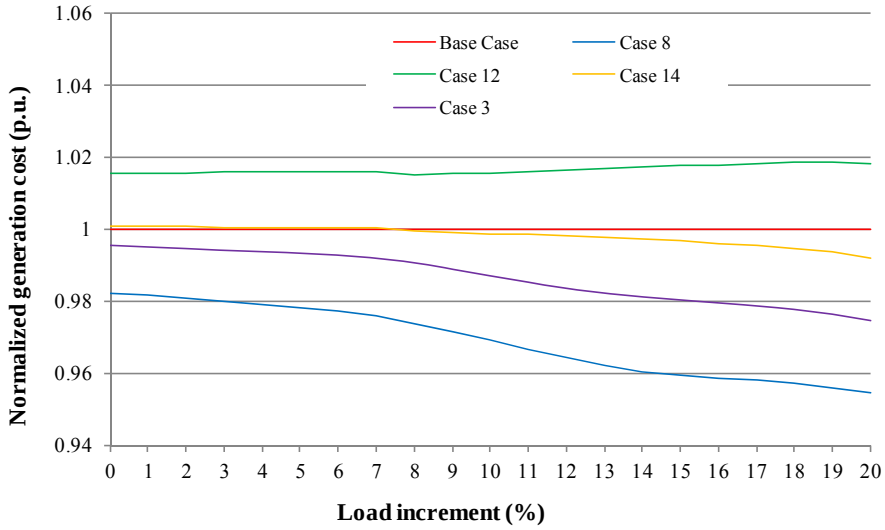

Figure 5.5. Normalized generation cost of selected cases in different load conditions.

As can be seen, the normalized generation costs decrease when the system is further stressed, which means that more generation costs can be reduced by using VSC-MTDC system in a stressed system compared to those of the Base Case. Among all cases, the generation costs of Case 8 are always lower than those of other cases. Case 12 shows almost same generation cost level for all load conditions compared to other cases because of the same reason discussed above. Two dc cables connect to one VSC station, and share its capacity. The capacity of this VSC station has been fully utilized, and cannot transfer more hydro power from the North to the Central area when the system is further stressed. Meanwhile, the VSC-MTDC system in Case 12 is located in the right side of two transmission corridors, which limits its reactive power support to the ac transmission lines on the left side of the corridor.

The comparison of the base case and Case 8 about the power generation in the North and the South areas, and the power transmitted between them are shown in Figure 5.6. It can be seen that the active power transmitted from the North to the South is increased about 300 MW by using VSC-MTDC. Meanwhile, the power generated in the North and the South has the corresponding changes. This is the

main reason that more low cost hydro power can be utilized when the VSC-MTDC system is used in Case 8.

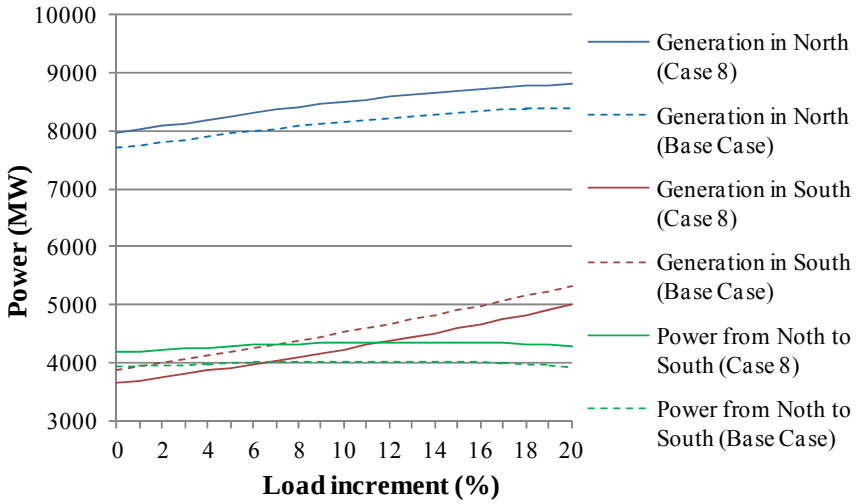

Figure 5.6. Comparison of power generation and transmission of two cases.

5.2.2 Impact of the Considered VSC Station Loss Ratio

The sensitive analysis of the generation cost to different VSC station loss ratios is carried out for the selected cases. Figure 5.7 shows the results. The loss ratio of the VSC station is reduced from 1.8 % to 0.6 % of the VSC rating in the nominal load condition. The loss ratio of 1.8 % is the general used value of a two-level VSC station [118], while the loss ratio of 0.6 % is the assumed loss level of the future VSC station. As can be seen, the generation costs of all cases decreased with the decrease of the VSC station loss ratio. However, when the VSC station loss ratio is reduced more than about 60 % from 1.8 % to 0.6 %, the generation costs of all these selected cases are only decreased about 0.5 %, which shows that the generation cost is not sensitive to the VSC station losses.

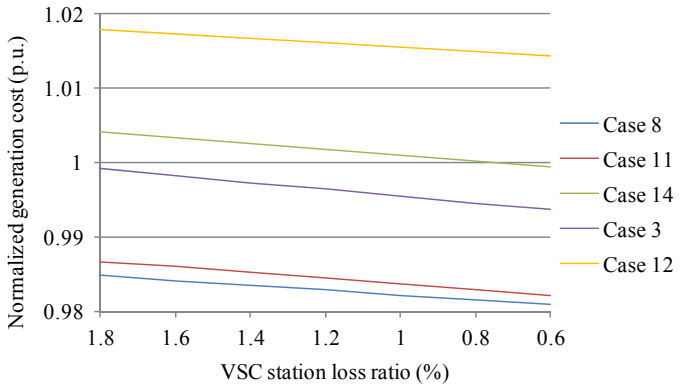

Figure 5.7. Normalized power generation cost of selected cases in different VSC station loss ratio.

5.3 Power loss reduction analysis

5.3.1 Results and Discussions

The M-OPF model is applied to the same cases designed in Section 5.1.2 with the objective function to minimize the overall system losses. The power losses of all cases at the nominal load level are shown in Figure 5.8, which are normalized over the power loss of the Base Case.

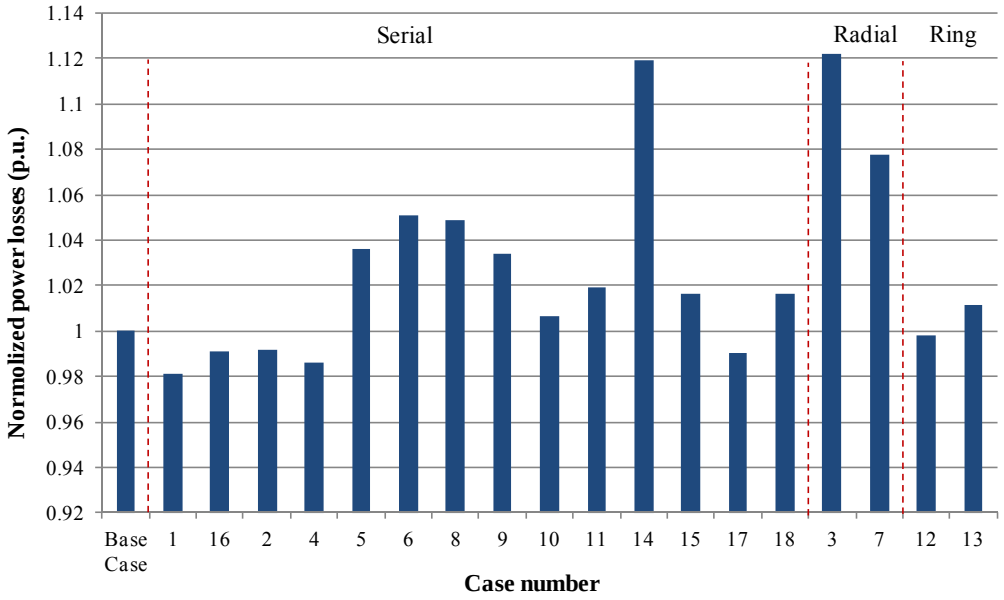

Figure 5.8. Normalized system power losses.

As can be seen from Figure 5.8, 6 of all 18 modified cases have the lower system losses than that of the Base Case, and the other cases show opposite results. Therefore, it is clear that not all VSC-MTDC systems can help the ac grid to reduce the overall system losses even when the ac transmission lines with high power losses are replaced by the equivalent dc links. Among all cases, Case 1 and Case 4 have the lowest power losses, and Case 14 and Case 3 show the highest power losses.

The detailed results from the seven selected cases are shown in Figure 5.9, Figure 5.10, and Table 5.4. Figure 5.9 compares the voltages of some selected buses in the seven cases. As can be seen, the voltages of selected buses in the Base Case are much lower than those of the other four cases (Case 1, 3, 4 and 13). Figure 5.10 shows the power loss components of the seven cases. It can be seen that the total losses through ac lines and dc cables are reduced when the VSC-MTDC systems are used. However, VSC stations introduce the extra losses which make the overall system losses of some cases higher than that of the Base Case. Table 5.4 presents the power flow changes of the selected ac lines connecting generation and load centers before and after the VSC-MTDC systems are embedded. The

transferred power through those heavily loaded ac lines are reduced when dc cables are connected in parallel. Thus, their power losses are reduced as well.

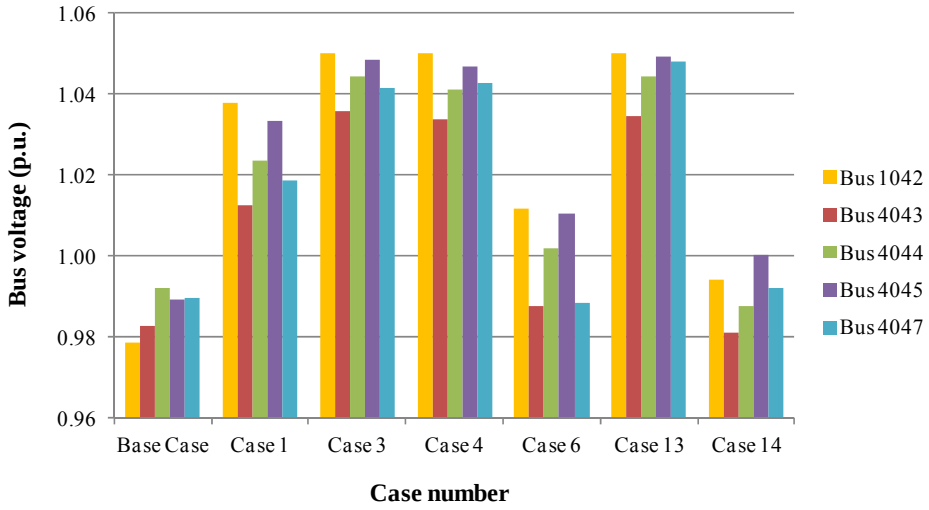

Figure 5.9. Comparison of voltages of selected buses in seven cases.

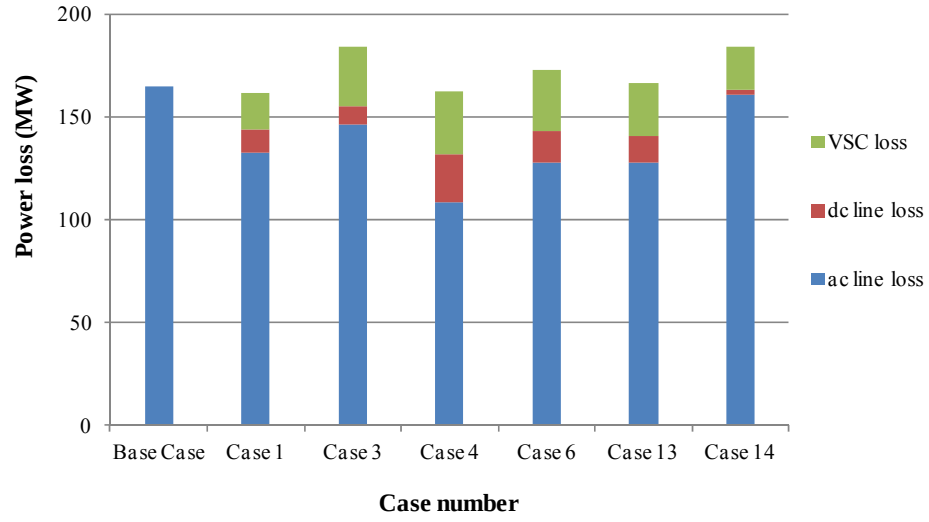

Figure 5.10. Comparison of power losses of selected cases.

Table 5.4 Comparison of Transferred Power (MW)

Line	Base Case	Case 1	Case 3	Case 4	Case 6	Case 13	Case 14
4044 - 4032	405	687*	540	731*	374	592*	408
4041 - 4031 (Line 1)	385	331	406	321	578*	331	390
4041 - 4031 (Line 2)	385	331	406	321	284	331	390
4041 - 4031 (Total)	770	662	812	643	862	662	781
4042 - 4021	360	312	336	263	334	306	361
4042 - 4032	296	170	148	192	269	279*	300

The values marked with * are the power flow of dc cables

From the above analysis, it can be concluded that the reduction of power losses by using VSC-MTDC systems is due to three main reasons: 1) The bus voltages are increased by having more reactive power support from VSCs, especially in the load area; 2) The power losses of dc links are lower than those of corresponding ac lines; 3) The loading levels on ac transmission lines in parallel with the dc links are reduced. However, because of the extra losses from VSC stations, the effect of VSC-MTDC systems in reduction of system losses depends on the trade-off between the reduced power losses from ac transmission lines by embedding dc links and the extra losses introduced by VSCs stations.

The normalized system losses of the selected cases at different load levels are shown in Figure 5.11. The system load is increased equally at all load busses by 1 % of each increment up to 118 % of the nominal load level. The losses are normalized over the corresponding system loss of the Base Case at the same load condition, which means that the system losses of the Base Case at all load conditions are normalized to 1 p.u..

It can be seen from Figure 5.11, when stressing the system by evenly increasing the load on each buss step by step, the normalized losses of the modified cases decreased continually compared to the Base Case, except the Case 13. This is due to the fact that more power is needed from the North to meet the increased load demand in the South, and the VSC-MTDC systems connecting the North and the South areas can share more power flow from parallel ac lines. Therefore, more system losses are reduced by the embedded VSC-MTDC system when the system is stressed. Case 4 is a typical example showing the power shift from ac lines to dc cables according to the data in Table 5.4 and Figure 5.11. In contrast, Case 13 is an opposite example due to the “Ring” configuration of the VSC-MTDC system. As discussed in Section 5.2, two dc cables connect to one VSC station in Case 13, which limits the fully utilization of the transmission capacity of dc cables. When the system is stressed, more power is needed to be transferred from the North to the Central area through ac transmission lines instead the dc cables. In other words, the total system power losses increase when the system load increases.

5.3.2 Impact of the Considered VSC Station Loss Ratio

According to the above discussion, the power loss ratios of VSC stations play an important role in the reduction of system power losses. To test how the system loss will be affected by the VSC power loss ratio, a sensitivity analysis was carried out using same four selected cases in the nominal load condition. The VSC station loss ratio is decreased from 1.8 % to 0.6 % of the VSC rating, as assumed in Section 5.2. The analysis results are shown in Figure 5.12.

As can be seen the system losses of all six modified cases decrease with the decrease of the VSC station loss ratio. When the loss ratio is 1.8 %, the system losses of all six cases are higher than that of the Base Case. Therefore, the embedded VSC-MTDC system cannot help ac grid to reduce the power losses in

such VSC loss ratio level. As already discussed before for the case of VSC loss ratio of 1 %, the system losses might be reduced by the embedded VSC-MTDC systems in some cases depending on their configurations and locations. If the power loss ratio of the VSC station could be further decreased to 0.6 %, the system power losses of all four cases are found to be lower than that of the Base Case. Especially the VSC-MTDC system in Case 4 can help the ac grid to reduce about 10 % of system losses.

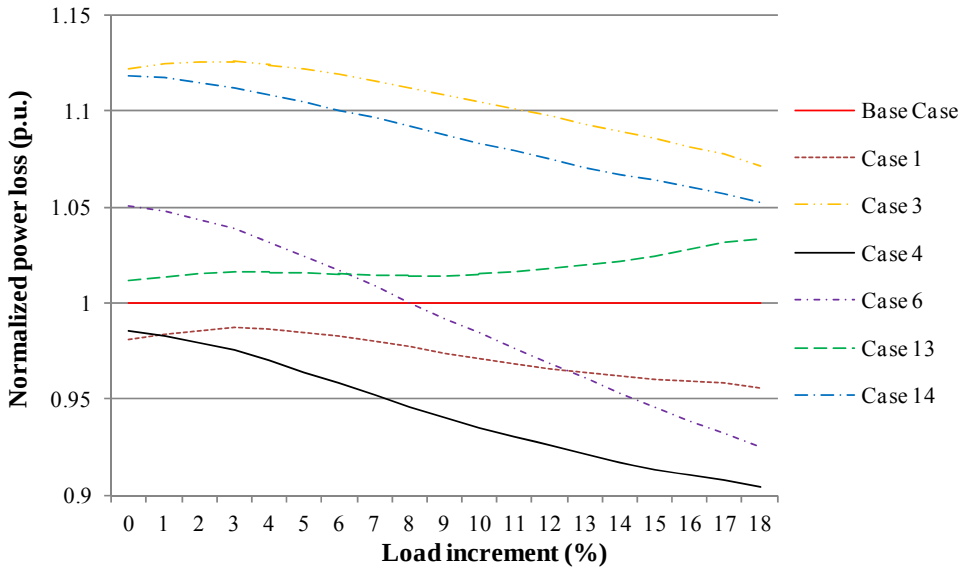

Figure 5.11. Normalized power losses of selected cases in different load conditions.

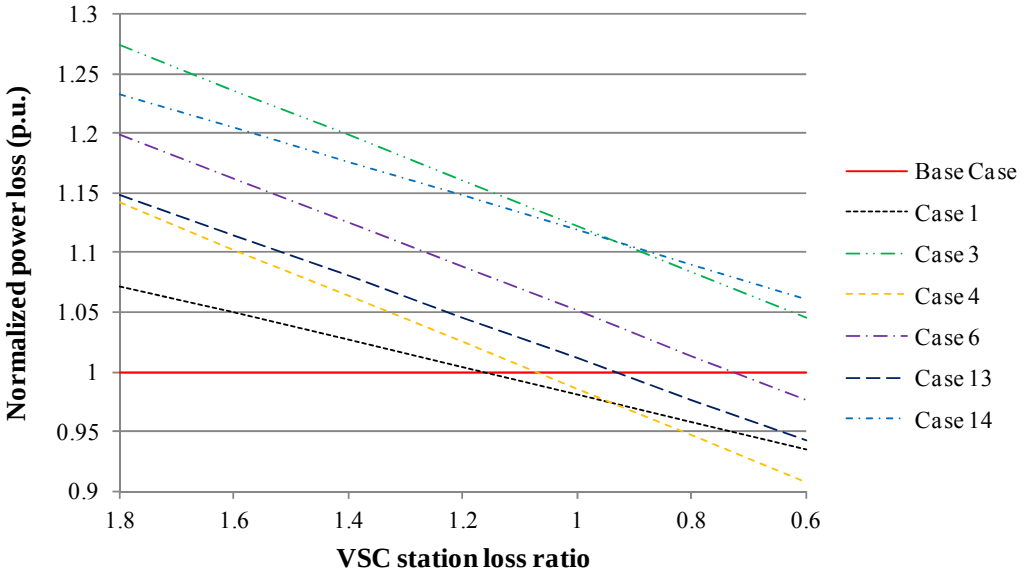

Figure 5.12. Normalized power losses of some typical cases in different VSC loss ratio.

5.4 Summary

The capabilities of proposed VSC-MTDC systems in the reduction of the system generation cost and the transmission losses are analyzed using the proposed M-OPF model applied to the Nordic 32-bus system. The results show:

- The reduction of the system generation cost and the transmission losses by VSC-MTDC depends, mainly, on the configuration and the location of the VSC-MTDC system.

- The characteristic of the power transmission of the Nordic 32-bus system is another important factor which affects the performance of the VSC-MTDC systems. The VSC-MTDC systems connecting the generation area in the North and the load center in the Central and the South usually can reduce the generation cost; VSC-MTDC systems which effectively supply extra reactive power support to the load center in the Central area and mitigate the heavily loaded ac transmission lines between the North and the Central might reduce the power transmission losses.

- When the transmission system is further stressed, the performances of all VSC-MTDC systems are diverse. Most of them can reduce more generation cost and power transmission losses, whereas a few of them show opposite performance.

- The power transmission losses are sensitive to the considered VSC loss ratio. The transmission losses are further reduced with the decrease of the VSC loss ratio. One extreme example is that the transmission losses can be reduced by about 10 % in Case 4 by using VSC-MTDC system if the VSC loss ratio is about 0.6 %.

Chapter 6

Cost-Benefit Analysis

In this chapter, a cost-benefit analysis approach using the M-OPF model, described in Chapter 4, is proposed to evaluate the benefits of the VSC-MTDC systems embedded in an existing ac transmission grid over the planning. This approach is applied on the Nordic 32-bus system in which VSC-MTDC system is embedded. The benefit-to-cost ratios of the VSC-MTDC alternatives are calculate, and are used to rank the alternatives of the VSC-MTDC systems according to their economic performance in the case study. The economically preferred VSC-MTDC candidates with the highest Benefit to Cost (BCR) values were identified. Sensitive analyses are also conducted to evaluate the influences of different VSC technologies on the benefits.

6.1 Cost-Benefit approach

The total economic benefit due to the VSC-MTDC system is defined as the sum of the reduction of the system generation cost and the reduction of the cost of the active power losses of the system compared to the Base Case without the deployment of the VSC-MTDC system. The present value of the total economic benefit is calculated for a whole planning period using (6-1).

$$TB = \sum_{yr=1}^{30}\left(PVF^{yr} \sum_{p=1}^{4}\left(t\left(C_1^{yr.p} - C_2^{yr.p} \right) + \Pr^{yr.p}\, t(L_1^{yr.p} - L_2^{yr.p}) \right) \right) \tag{6-1}$$

$$PVF^{yr} = 1/\left(1+r\right)^{yr-1} \tag{6-2}$$

The annual system load growth is assumed to be 0.5% over a period of 30 years. Each year is divided into four equal periods. The load coefficients of four periods are calculated based on typical peak load values for each period in Sweden in 2011 [117] and are provided in Table 6.1. The coefficients of these periods are used to calculate the load level in each period in each year.

Table 6.1. Load Coefficients

Period	Jan - Mar	Apr - Jun	Jul - Aug	Oct - Dec
Coefficient	1.00	0.76	0.64	0.84

The power price is estimated using unconstrained OPF [109] on the basis of the modified system load at season *p* and year *yr*. The objective of this unconstrained OPF is to minimize the generation cost.

The calculation process for the total economic benefit is shown in Figure 6.1. In the calculation, for each of the candidate VSC-MTDC systems, the M-OPF model is executed with the objective function (4-10), i.e., the minimization of the total system cost for the base case and for the case with selected VSC-MTDC system. Each model run provides the total generation costs and total system losses simultaneously for the cases considered. The total loss is converted to the cost of total loss by multiplying the power price calculated using the same M-OPF model run but without the transmission constraints (unconstrained case). It has been assumed that the compensated power due to losses has to be purchased at the unconstrained market price. The difference between the total costs in the two cases with and without VSC-MTDC represents the economic benefits of each alternative considered. The BCR as expressed in (6-3) is calculated for each of the candidate VSC-MTDC systems.

$$BCR = TB / Inv \tag{6-3}$$

The investment cost of the VSC-MTDC system, including the cost of VSC station equipment and DC cables for each case, is estimated by linearly scaling the investment of one project presented in [119] and shown in Table 6.2. The maintenance cost of VSC-MTDC is not taken into account.

Table 6.2. Unit Cost of VSC Station and DC Cable

Item	Unit	Cost	Device Parameter
VSC station	1 station	283 M$	1000 MVA, ±300 kV
HVDC Cable	1 km	0.7 M$	Land cable, 2000 mm^2, ±300 kV

6.2 Cost-Benefit analysis

The case study to evaluate the economics of all VSC-MTDC candidates using the proposed cost-benefit approach are carried out using the same cases designed in Section 5.1. The discount rate used in this study is assumed to be 8 %. The selection of the discount rate is a rather complex issue involving the weighted average cost of capital and the risks of the projects. As suggested in [120], the lower discount rate would often be chosen for the low risk project (could be smaller investment) while the higher discount rate would be chosen for the high risk project (could be larger investment). The VSC station power loss ratio at the nominal condition is assumed to be 1 % of the nominal VSC rating as suggested in [28]. The calculated total benefits of all the cases are shown in Figure 6.2. It is noted that the results are calculated for 30 years.

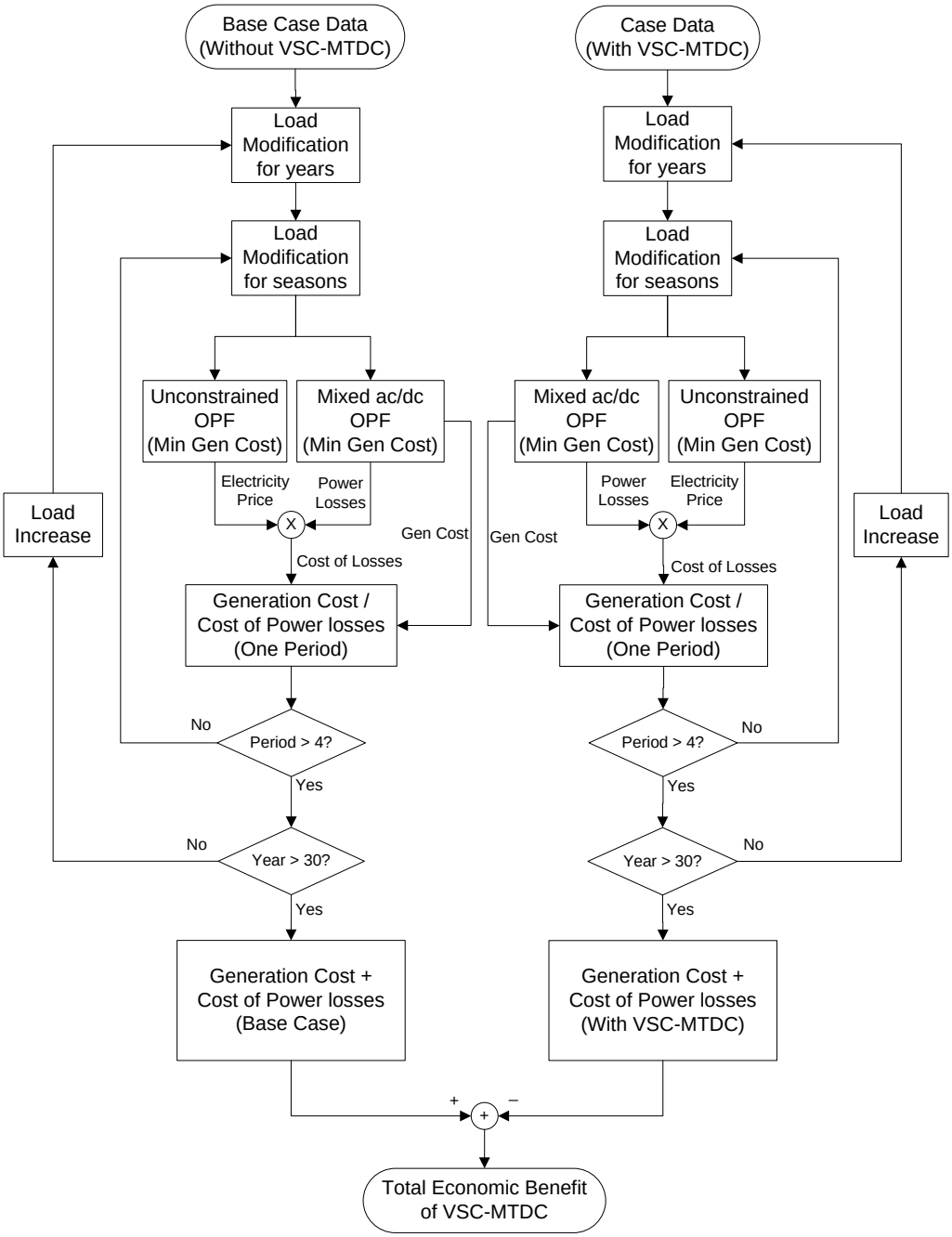

Figure 6.1. The proposed approach for the total economic benefit calculation.

As can be seen in Figure 6.2, 11 out of 18 modified cases have shown positive total benefits from using VSC-MTDC systems. The cases with high total benefits correspond to the "serial" topology type of VSC-MTDC, while all the cases using the ring topology of the VSC-MTDC system show negative benefits. This could be due to the fact that the same rating is used for all VSC stations. When two dc links are connected to one VSC station in the cases using ring topology type, they are limited by the capacity of that VSC station. Therefore, the capacity of these

two dc links cannot be fully utilized. Case 8 appears to have the highest total benefit because it has the highest reduction in total generation cost, even though it has the negative reduction cost of power loss (i.e., increase in the cost of loss). This might be attributed to the fact that the VSC-MTDC system in Case 8 connects the generation area in the North with the load area in the South. Since the power flow through the dc links in this case is controlled at their highest capacities, the total power transmission from North to South is increased compared to that in the Base Case with only ac transmission lines. Therefore, the total generation cost is reduced because more hydro power generation can be used. On the other hand, the VSC station introduces more power loss with the transmission of high power which results in higher system power loss in this case than that of the Base Case.

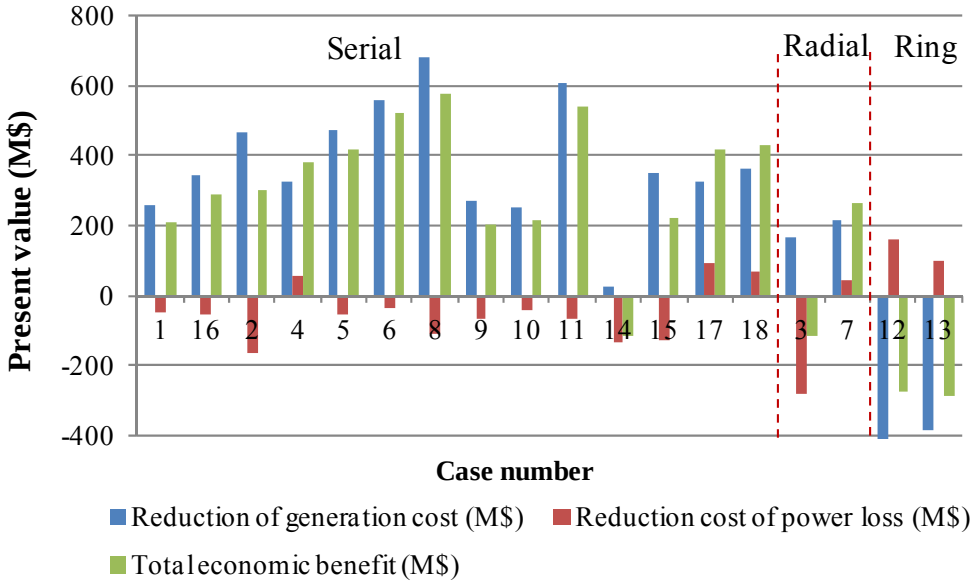

Figure 6.2. The present value of the reduction of generation cost, the reduction of costs of power loss, and the total economic benefit.

Figure 6.3 shows the calculated "Benefit-to-cost" ratios (BCRs) for all cases. The BCRs reflect the economic performance of the alternatives considered in terms of system cost reduction for every dollar of investment.

It can be seen in Figure 6.3 that Case 5, Case 8, and Case 11 have the highest BCR which are, therefore, the preferred cases from an economic benefits perspective. It is interesting to see that even though the total benefits of Case 5 and Case 11 are lower than that of Case 8, the low investment costs of these two cases make them having the same BCRs as Case 8. However, the BCRs for all cases are found to be lower than one and some of them are even negative, which means the total benefits considered in this study by utilizing VSC-MTDC are lower than its investment cost. It should be noted that this study focuses on analyses in the steady state. The other technical benefits in dynamic state,

including the improvement of system controllability and dynamic performance, are beyond the scope of the present study. In addition, the transmission charge could be considered a source of income from the project. This will be subject of future work. If such benefits could be considered, it should be expected that the BCRs would be much higher. Therefore, BCR is only one of the "performance indicators" which should be considered in selecting VSC-MTDC projects.

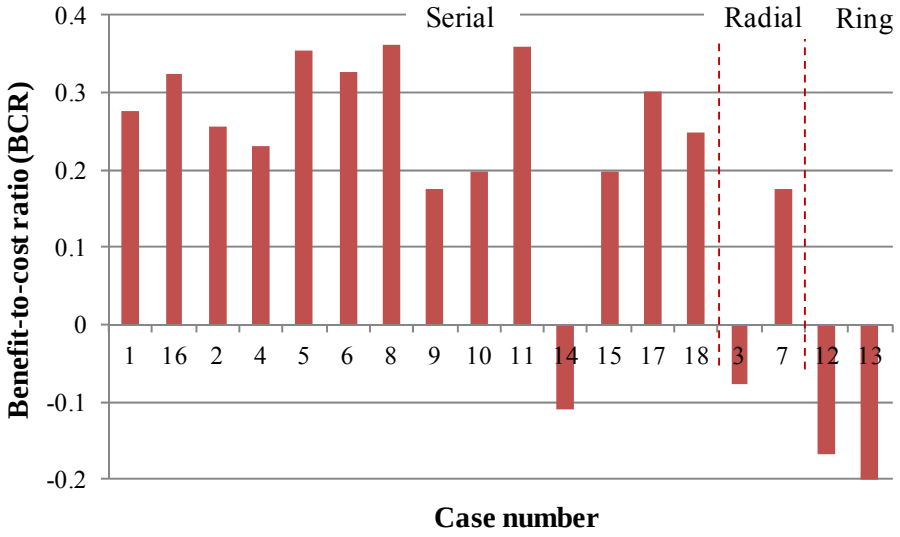

Figure 6.3. The Benefit-to-Cost Ratios of VSC-MTDC candidates.

In order to understand how the results, i.e., the total benefits, would vary with changes of the economy and the technologies of VSC-MTDC systems, sensitivity analyses have been performed with regard to the changes in the discount ratio, the nominal capacity and the VSC losses for the three selected Cases 5, 8, and 11. Figure 6.4 and Figure 6.5 shows the changes of the reduced generation cost, reduced power loss cost, total benefit and BCR values with three different discount ratios. As can be seen, when the discount ratio changes from 8% to 5%, the reduction of generation costs and the reduction of power loss costs in all the three cases increase by about 36% on average, which results in the respective changes of the total benefit. On the contrary, all these values decrease by about 16% when the discount ratio increases from 8% to 10%. Meanwhile, the investment costs of VSC-MTDC systems in this study won't be affected by the discount ratio since they are considered as one-time investment. Therefore, the BCR values of the three cases shown in Figure 6.5 still have almost the same values with different discount ratios.

Figure 6.6 shows the changes of total benefits of the three cases with regard to the changes of the VSC station nominal capacity and its loss ratio. As can be seen, when the capacity of the VSC-MTDC system is increased by 20%, from 1000 MW to 1200 MW (the dc cable conductor area is changed to 2200 mm^2), the total benefits for all the three cases are increased by about 50% when the VSC loss is 1%

of the nominal VSC capacity, and by about 75% or 45% when the VSC loss is 1.8% or 0.6%, respectively. When the VSC loss ratio is increased to 1.8%, the total benefits for all the three cases are decreased by about 35% for the VSC capacity of 1000 MVA. However, if the VSC loss ratio could be reduced to 0.6%, the total benefits of these three cases could be increased by about 15%. The BCRs have not been calculated in the sensitivity analyses because the estimation of the costs of the VSC having lower losses (e.g., 0.6%) is not determined yet. It is clear that Case 8 still remains the preferred alternative for the VSC-MTDC system.

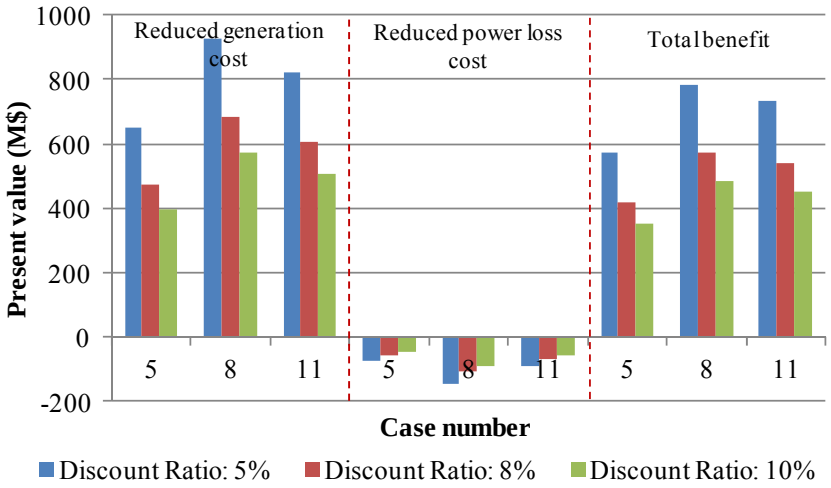

Figure 6.4. Changes in reduced generation cost, reduced power loss cost, and total benefit with different discount ratio.

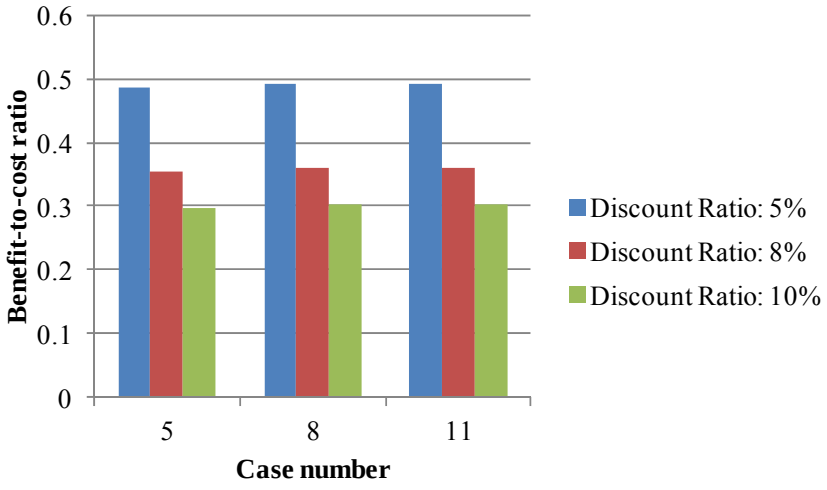

Figure 6.5. Changes in benefit-to-cost ratio (BCR) with different discount ratio.

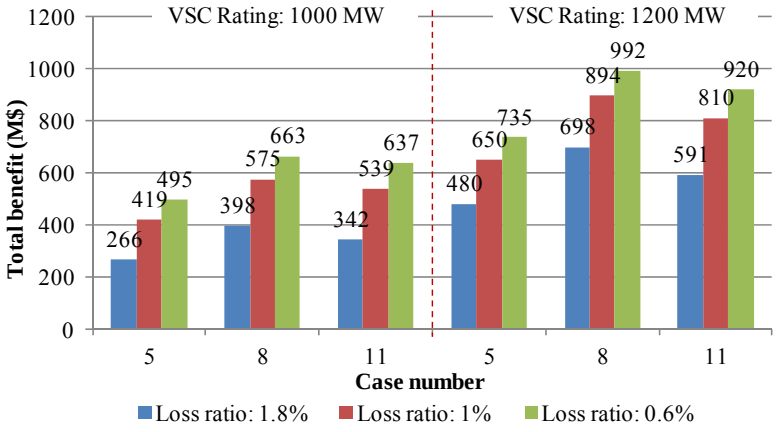

Figure 6.6. Changes in the total benefit with different VSC station capacities and loss ratios

6.3 Summary

In this chapter, a cost-benefit analysis approach of the VSC-MTDC systems embedded in the ac transmission grid is proposed using the extended OPF model incorporating VSC-MTDC system. A case study has been carried out using the Nordic 32-bus system. The benefit-to-cost ratios of the VSC-MTDC alternatives were calculated. The economically preferred VSC-MTDC systems with the highest BCR values were identified. The case study results showed that the systems with relatively high benefits may not necessarily have the high BCR values. To gain a more comprehensive picture of the total benefits rendered by VSC-MTDC projects, additional technical benefits have to be evaluated and will be the subject of further investigations, e.g., utilizing the independent control of active and reactive power of the VSC stations.

Chapter 7

Conclusions and Future Work

This chapter summarizes the research work in this thesis, and provides conclusions and findings of the study results. The future work in this thesis is also described.

7.1 Conclusions

The thesis has focused on the analysis of the potential benefits provided by embedded VSC-MTDC systems at the steady-state operation of the transmission grid. The potential benefits were identified as reduction of the generation cost and transmission losses. The following models and approach were developed to evaluate the possible benefits, and therefore to assess the economics and performance of the VSC-MTDC systems embedded in a traditional ac transmission grid.

- A detailed steady-state model of the VSC-MTDC system. The dc power flow equations were included in the model and the VSCs were treated as the power "exchanger" between ac and dc grids. The fundamental technical limits of VSC (the maximum VSC valve current and the maximum dc voltage) were used as the operation constraints of VSC stations.

- A Mixed ac/dc grid Optimal Power Flow (M-OPF) model for the mixed ac/dc grid based on the VSC-MTDC systems. The traditional ac OPF model was extended to incorporate the developed steady-state VSC-MTDC model. Two objective functions of the M-OPF model were minimization of the generation cost and minimization of the transmission losses. The constraints of ac grid and VSC-MTDC systems were adopted, and ac and dc power flow equations can be solved simultaneously.

- A cost-benefit approach using M-OPF model as a calculation "engine" is proposed to evaluate the economics of different VSC-MTDC alternatives which are considered in the transmission expansion planning. In this approach, the benefit is defined as the sum of the avoided generation cost and avoided cost of transmission losses by using VSC-MTDC system. The

cost includes the investment cost of the underground dc cables and the VSC stations. The Benefit-to-Cost Ratio (BRC) is used to rank the economics of all VSC-MTDC system alternatives, which has led to identification of the preferred candidate.

Case studies were carried out using the proposed M-OPF model and Nordic 32-bus system to analyze the capability of VSC-MTDC systems in reduction of the generation cost and the transmission losses. The cost-benefit analysis using the proposed cost-benefit approach was conducted as well using the same study cases to evaluate the economics of all VSC-MTDC alternatives. The main results from the case studies can be concluded as follow:

- VSC-MTDC systems might lead to reductions in generation cost and transmission losses depending on their configurations and locations.

- The reduction in generation cost is mainly due to the facts that VSC-MTDC systems can supply higher transmission capacity compared to the corresponding ac transmission lines, and increasing the transmission capacity of the ac transmission lines by providing reactive power support from VSC stations. Therefore, the utilization of the low cost generations is enhanced, and the total generation cost is reduced.

- The reduction in system transmission losses is a trade-off result between the reduced power losses from ac transmission lines by embedding VSC-MTDC systems and the extra losses introduced by VSC stations. The losses of ac lines could be reduced by increasing bus voltages because of the reactive power support from VSC stations and by mitigating their heavy power flow by the parallel dc cables. However, in some cases, the power losses of VSC stations are relatively high compared to the reduced ac transmission losses which make the total system power losses even higher than the original ac transmission system.

- The total benefits from using VSC-MTDC systems also depend on the configurations and the locations of the VSC-MTDC alternatives. This is because they are dominated by the avoided generation cost in most of cases. On the other hand, when considering both benefits and investment costs, the VSC-MTDC alternatives with relatively high benefits may not necessarily have the high BCR values.

- Sensitive analyses show that the transmission losses and total benefit are sensitive to the power loss ratios of VSC stations. If VSC station loss ratio could be lowered to 0.6% in the nominal condition, the total system loss could be reduced by 10% in one study case, and the total benefit would be increased by about 70% in another case.

7.2 Future work

The thesis focused on the benefit evaluation from using embedded VSC-MTDC systems in the steady state. The evaluated benefits include the avoided generation cost and the avoided transmission losses. However, these are only a small part of the benefits rendered by VSC-MTDC systems. To obtain a more complete picture, the benefits evaluation should be put into a wider framework of the electric power market, in which the social welfare could be an assessment index of VSC-MTDC alternatives. Meanwhile, the benefits provided by VSC-MTDC systems in dynamic operation of the electric transmission grid are other crucial aspects which should be evaluated and accounted into the total benefit. For example, the fast response of both the active and reactive power control of VSC-MTDC systems can improve the transient and voltage stability of the system operation. Therefore, the following aspects are some of the recommendations for future work.

- Improve the M-OPF model by adding other constraints, e.g., the voltage stability constraints. Thus, the system operation can be more realistically simulated, and more reasonable results can be obtained.

- Combine the electric power market model and the M-OPF model to evaluate the benefits from VSC-MTDC systems in terms of the social welfare. For example, the impact of VSC-MTDC systems on mitigating the transmission congestion, and therefore reducing the social cost.

- Investigate the dynamic interaction between ac and VSC-MTDC systems to understand the benefits from using VSC-MTDC systems in the improvement of the system stability and reliability.

- Propose an operation strategy for the mixed ac/dc transmission grid on the basis of the VSC-MTDC system.

Appendix A

Table A-1. Example of VSC-HVDC projects

Project Name	Year	Power rating	Circuit Number	AC voltage	DC voltage	Length of DC line	Comments and reasons for choosing VSC-HVDC	Topology
Hellsjön, Sweden	1997	3 MW, ±3 MVAr	1	10 kV (both ends)	±10 kV	10 km Overhead line	Test transmission. Synchronous AC grid.	2-level
Gotland HVDC light, Sweden	1999	50 MW, -55 to +50 MVAr	1	80 kV (both ends)	±80 kV	2×70 km Submarine Cable	Wind power (voltage support). Easy to get permission for underground cables.	2-level
Eagle Pass, USA	2000	36 MW, ±36 MVAr	1	138 kV (both ends)	±15.9 kV	Back-to-back station	Controlled asynchronous connection for trading. Voltage control. Power exchange.	3-level
Tjäreborg, Denmark	2000	8 MVA, 7.2 MW, -3 to +4 MVAr	1	10.5 kV (both ends)	±9 kV	2×4.3 km Submarine cable	Wind power. Demonstration project. Normally synchronous ac grid with variable frequency control	2-level
Terrenora Interconnection (Directlink), Australia	2000	180 MW, -165 to +90 MVAr	3	110 kV(Bungalora) 132 kV (Mullumbimby)	±80 kV	6×59 km Underground cable	Energy trade, Asynchronous AC grid. Easy to get permission for underground cables	2-level

Project Name	Year	Power rating	Circuit Number	AC voltage	DC voltage	Length of DC line	Comments and reasons for choosing VSC-HVDC	Topology
MurrayLink, Australia	2002	220 MW, -150 to +140 MVAr	1	132 kV (Berri) 220 kV (Red Cliffs)	±150 kV	2×180 km Underground cable	Controlled asynchronous connection for trading. Easy to get permission for underground cables	3-level ANPC
CrossSound, USA	2002	330 MW, ±150 MVAr	1	345 kv (NewHeaven) 138 kV (Shoreham)	±150 kV	2×40 km Submarine cable	Controlled asynchronous connection for power exchange. Submarine cables	3-level ANPC
Troll A offshore, Norway	2005	84 MW, -20 to +24 MVAr	2	132 kV (Kollsnes) 56 kV (Troll)	±60 kV	4×70 km Submarine cable	Environment, CO_2 tax. Long submarine cable distance. Compactness of converter on platform electrification.	2-level
Estlink, Estonia-Finland	2006	350 MW, ±125 MVAr	1	330 kV (Estonia) 400 kV (Finland)	±150 kV	2×31 km Underground 2×74 km Submarine	Length of land cable, sea crossing and asynchronous AC systems	2-level
NORD E.ON 1, Germany	2009	400 MW	1	380 kV (Diele) 170 kV (Borkum 2)	±150 kV	2×75 km Underground 2×128 km Submarine	Offshore wind farm to shore. Length of land and sea cables. Asynchronous system.	
Caprivi Link, Namibia	2009	300 MW	1	330 kV (Zambezi) 400 kV (Gerus)	350 kV	970 km Overhead line	Synchronous AC grids. Long distance overhead line, connecting two weak networks	

Project Name	Year	Power rating	Circuit Number	AC voltage	DC voltage	Length of DC line	Comments and reasons for choosing VSC-HVDC	Topology
Valhall offshore, Norway	2009	78 MW	1	300 kV (Lista) 11 kV (Valhall)	150 kV	292 km Submarine coaxial cable	Reduce cost and improve operation efficiency of the field. Minimize emission of green house gases	2-level
Trans Bay Cable, USA	2010	400 MW, ±170 MVAr	1	230kV (Pittsburg) 138 kV (San Francisco)	±200 kV	88 km Submarine cable	Provide reliable energy to San Francisco without having to install a power generation plant.	MMC
BorWin2, Germany	2013 (scheduled)	800MW		150kV (offshore) 400kV (Diele)	300 kV	125 km offshore, 75km onshore	Two offshore wind farms to onshore. Capacity of VSC-HVDC	MMC
HelWin1, Germany	2013 (scheduled)	576MW		155kV (offshore) 259 (Büttle)	250 kV	130 km	Integrate offshore wind farms to onshore grid.	MMC
INELFE	2013 (scheduled)	2×1000 MW	2	400kV (Baixas, France) 400kV (Santa Llogaia, Spain)	±320 kV	4×32 km Span + 4×33 km France underground cable	Transport large amount of electric power with a minimum of transmission losses	MMC
South West link	2014	South part: 2×600 MW	2	400 kV	±300 kV	South part: 4×180 km underground cable + 70 km overhead line	Planned as a three-terminal VSC-HVDC links, high transmission capacity	MMC

Appendix B. Parameters of the 6-bus System

Table B-1. Generation and load data

Bus	Generation Capacity, MW	Generator Cost Characteristic, $/hr	Load (MW+jMVAr)	Voltage, p.u.	Reactive support, MVAr
1	$100 \le P_1 \le 400$	$P_1 + 8.5\ P_1 + 5$	48.75 + j 13.00	1.05	$-20 \le Q_1 \le 300$
2	$50 \le P_2 \le 200$	$3.4P_2 + 25.5\ P_2 + 9$	61.75 + j 19.50	0.06	$-20 \le Q_2 \le 150$
3	-	-	52.00 + j 26.00	$0.9 \le V_3 \le 1.1$	-
4	-	-	74.75 + j 20.80	$0.9 \le V_4 \le 1.1$	$0 \le Q_4 \le 100$
5	-	-	84.50 + j 22.75	$0.9 \le V_5 \le 1.1$	-
6	-	-	35.75 + j 16.25	$0.9 \le V_6 \le 1.1$	$0 \le Q_6 \le 100$
Total			550 + j 177.45		

Table B-2. System network data

From Bus to Bus	Resistance, R (in p.u.)	Reactance, X (in p.u.)	Line Charging, $y_{i,j}/2$ (in p.u.)
1 - 4	0.0662	0.1804	0.003
1 - 6	0.0945	0.2987	0.005
2 - 3	0.0210	0.1097	0.004
2 - 5	0.0824	0.2732	0.004
3 - 4	0.1070	0.3185	0.005
4 - 6	0.0639	0.1792	0.001
5 - 6	0.0340	0.0980	0.004

References

[1] "The early HVDC development," Grid Systems HVDC, ABB AB, [Online]. Available: http://www.abb.com

[2] "Jinping - Sunan 7200 MW UHVDC transmission," ABB, [Online]. Available: http://www.ng.abb.com/industries

[3] U. Axelsson, A. Holm, C. Liljegren, K. Eriksson, and L. Weimers, "Gotland HVDC light transmission - world's first commercial small scale dc transmission," in *CIRED Conference 1999*, Nice, May 1999.

[4] M. Byggeth, K. Johannesson, C. Liljegren, and U. Axelsson, "Gotland HVDC Light - The World's First Commercial Extruded HVDC Cable System," in *CIGRÉ 2000*, Paris, France, August, 2000.

[5] U. Axelsson, A. Holm, C. Liljegren, M. Aberg, K. Eriksson, and O. Tollerz, "The Gotland HVDC Light Project - Experiences from Trial and Commercial Operation," in *CIRED 2001*, Amsterdam, June, 2001.

[6] T. Nakajima and S. Irokawa, "A control system for HVDC transmission by voltage sourced converters," in *Power Engineering Society Summer Meeting, 1999. IEEE*, 1999, pp. 1113-1119 vol.2.

[7] "It's time to connect - A technical description of HVDC Light®," ABB AB, Grid Systems - HVDC, [Online]. Available: http://www.abb.com

[8] B. Jacobson, B. Westman, and M. P. Bahrman, "500 kV VSC Transmission System for lines and cables," in *Cigre 2012 San Francisco Colloquium*, San Francisco, 2012.

[9] "The HVDC Transmission Québec - New England," ABB, [Online]. Available: http://www.abb.com/industries/ap/db0003db004333/87f88a41a0be97afc125774b003e6109.aspx

[10] J. Stefan G, A. Gunnar, J. Erik, and R. Roberto, "Power System Stability Benefits with VSC DC-transmission Systems," in *CIGRE Conference*, Paris, France, 2004.

[11] P. Jiuping, R. Nuqui, K. Srivastava, T. Jonsson, P. Holmberg, and Y. J. Hafner, "AC Grid with Embedded VSC-HVDC for Secure and Efficient Power Delivery," in *Energy 2030 Conference, 2008. ENERGY 2008. IEEE*, 2008.

[12] F. Mazzoldi, J. P. Taisne, C. J. B. Martin, and B. A. Rowe, "Adaptation of the control equipment to permit 3-terminal operation of the HVDC link between Sardinia, Corsica and mainland Italy," *IEEE Transactions on Power Delivery,* vol. 4, pp. 1269-1274, 1989.

[13] "Boosting Sweden's Transmission Capacity and Grid System Reliability, South-West HVDC Link, Sweden," ABB AB, High Voltage Cables, [Online]. Available: http://www.abb.com

[14] "The South West Link," Svenska Kraftnät (Swedish Transmission System Operator), [Online]. Available: http://www.svk.se/Start/English/Projects/Project/The-South-West-Link/

[15] K. Rudion, A. Orths, P. B. Eriksen, and Z. A. Styczynski, "Toward a Benchmark test system for the offshore grid in the North Sea," in *IEEE Power and Energy Society General Meeting, 2010*, Minneapolis, 2010.

[16] T. M. Haileselassie, M. Marta, and U. Tore, "Multi-Terminal VSC-HVDC System for Integration of Offshore Wind Farms and Green Electrification of

Platforms in the North Sea," in *NORPIE/2008, Nordic Workshop on Power and Industrial Electronics*, Helsinki, 2008.

[17] "Ten-year Network Development Plan 2010-2020," European Network of Transmission System Operators for Electricity (ENTSO-E), [Online]. Available: https://www.entsoe.eu/major-projects/ten-year-network-development-plan/tyndp-2010/

[18] "Energy infrastructure priorities for 2020 and beyond - A Blueprint for an integrated European energy network," European Commission, Belgium, 2011.

[19] "VSC transmission," CigreTech. Rep. Working Group B4.37-269, 2005.

[20] J. Gerdes. (2011) Siemens Debuts HVDC PLUS with San Francisco's Trans Bay Cable. *Living Energy*. Available: http://www.energy.siemens.com/hq/en/energy-topics/publications/living-energy/

[21] L. Jih-Sheng and P. Fang Zheng, "Multilevel converters - a new breed of power converters," *IEEE Transactions on Industry Applications,* vol. 32, pp. 509-517, 1996.

[22] N. Flourentzou, V. G. Agelidis, and G. D. Demetriades, "VSC-Based HVDC Power Transmission Systems: An Overview," *IEEE Transactions on Power Electronics* vol. 24, pp. 592-602, 2009.

[23] A. Nabae, I. Takahashi, and H. Akagi, "A New Neutral-Point-Clamped PWM Inverter," *IEEE Transactions on Industry Applications,* vol. IA-17, pp. 518-523, 1981.

[24] Z. Lidong, "Modeling and Control of VSC-HVDC Links Connected to Weak AC Systems," PhD Thesis, School of Electrical Technology, Electrical Machines and Power Electronics, Royal Institute of Technology, Stockholm, 2010.

[25] A. Lesnicar and R. Marquardt, "An innovative modular multilevel converter topology suitable for a wide power range," in *Power Tech Conference Proceedings*, Bologna, 2003.

[26] R. Marquardt, "Modular Multilevel Converter: An universal concept for HVDC-Networks and extended DC-Bus-applications," in *Power Electronics Conference (IPEC)*, Sapporo, Japan, 2010.

[27] S. Allebrod, R. Hamerski, and R. Marquardt, "New transformerless, scalable Modular Multilevel Converters for HVDC-transmission," in *IEEE Power Electronics Specialists Conference (PESC) 2008*, Rhodes, Greece, 2008, pp. 174-179.

[28] B. Jacobson, P. Karlsson, G. Asplund, L. Harnefors, and T. Jonsson, "VSC-HVDC Transmission with Cascaded Two-Level Converters," in *The 43rd CIGRE General Session 2010*, Paris, France, 2010.

[29] Alstom. (2011) HVDC-VSC: transmission technology of the future. *Think Grid*. Available: http://www.alstom.com/Global/Grid/Resources/Documents/Smart%20Grid/Think-Grid-08-%20EN.pdf

[30] D. Schmitt, Y. Wang, T. Weyh, and R. Marquardt, "DC-side fault current management in extended multiterminal-HVDC-grids," in *The 9th International Multi-Conference on Systems, Signals and Devices (SSD)* Chemnitz, Germany, 2012.

[31] R. Marquardt, "Modular Multilevel Converter Topologies with DC-Short Circuit Current Limitation," in *2011 IEEE 8th International Conference on Power Electronics - ECCE Asia (ICPE & ECCE)*, Jeju, Korea, 2011, pp. 1425-1431.

[32] M. Davies, M. Dommaschk, J. Dorn, J. Lang, D. Retzmann, and D. Soerangr. "HVDC PLUS - basics and principle of operation," [Online]. Available: http://www.energy.siemens.com/mx/en/power-transmission/hvdc/hvdc-plus/

[33] M. Ned, M. U. Tore, and P. R. William, *Power Electronics - Converters, Applications, and Design*: John Wiley & Sons, Inc., 2003.

[34] J. A. Houldsworth and D. A. Grant, "The Use of Harmonic Distortion to Increase the Output Voltage of a Three-Phase PWM Inverter," *IEEE Transactions on Industry Applications,* vol. IA-20, pp. 1224-1228, 1984.

[35] J. Jose, G. N. Goyal, and M. V. Aware, "Improved inverter utilisation using third harmonic injection," in *2010 Joint International Conference on Power Electronics, Drives and Energy Systems (PEDES) & 2010 Power India*, New Delhi, India, 2010.

[36] G. Eryong, S. Pinggang, Y. Manyuan, and W. Bin, "Selective Harmonic Elimination Techniques for Multilevel Cascaded H-Bridge Inverters," in *Power Electronics and Drives Systems (PEDS)*, Kuala Lumpur, Malaysia, 2005, pp. 1441-1446.

[37] M. S. A. Dahidah and V. G. Agelidis, "Selective harmonic elimination multilevel converter control with variant DC sources," in *The 4th IEEE Conference on Industrial Electronics and Applications (ICIEA), 2009*, Xian, China, 2009, pp. 3351-3356.

[38] S. Sirisukprasert, L. Jih-Sheng, and L. Tian-Hua, "Optimum harmonic reduction with a wide range of modulation indexes for multilevel converters," in *Industry Applications Conference, 2000*, Rome, Italy, 2000, pp. 2094-2099 vol.4.

[39] H. S. Patel and R. G. Hoft, "Generalized Techniques of Harmonic Elimination and Voltage Control in Thyristor Inverters: Part II -- Voltage Control Techniques," *IEEE Transactions on Industry Applications,* vol. IA-10, pp. 666-673, 1974.

[40] H. S. Patel and R. G. Hoft, "Generalized Techniques of Harmonic Elimination and Voltage Control in Thyristor Inverters: Part I -- Harmonic Elimination," *IEEE Transactions on Industry Applications,* vol. IA-9, pp. 310-317, 1973.

[41] Y. H. Liu, J. Arrillaga, and N. R. Watson, "Addition of four-quadrant power controllability to multi-level VSC HVDC transmission," *Generation, Transmission & Distribution, IET,* vol. 1, pp. 872-878, 2007.

[42] J. L. Thomas, S. Poullain, and A. Benchaib, "Analysis of a robust DC-bus voltage control system for a VSC transmission scheme," in *The 7th International Conference on AC-DC Power Transmission, 2001*, London, 2001, pp. 119-124.

[43] A. Yazdani and R. Iravani, "Dynamic model and control of the NPC-based back-to-back HVDC system," *IEEE Transactions on Power Delivery,* vol. 21, pp. 414-424, 2006.

[44] Z. Huang, B. T. Ooi, L. A. Dessaint, and F. D. Galiana, "Exploiting voltage support of voltage-source HVDC," *IEE Proceedings-Generation, Transmission and Distribution,* vol. 150, pp. 252-256, 2003.

[45] C. Du and M. H. J. Bollen, "Power-frequency control for VSC-HVDC during island operation," in *The 8th IEE International Conference on AC and DC Power Transmission (ACDC), 2006* London, 2006, pp. 177-181.

[46] F. Al Jowder and B. T. Ooi, "VSC-HVDC station with SSSC characteristics," in *IEEE Power Electronics Specialist Conference, 2003. PESC '03.* , 2003, pp. 1785-1791 vol.4.

[47] B. T. Ooi and X. Wang, "Voltage angle lock loop control of the boost type PWM converter for HVDC application," *IEEE Transactions on Power Electronics,* vol. 5, pp. 229-235, 1990.

[48] J. Svensson, "Simulation of power angle controlled voltage source converter using a linear quadratic method in a wind energy application," in *IEEE Workshop on Computers in Power Electronics*, Portland, USA, 1996, pp. 157-162.

[49] M. P. Kazmierkowski and L. Malesani, "Current control techniques for three-phase voltage-source PWM converters: a survey," *IEEE Transactions on Industrial Electronics,* vol. 45, pp. 691-703, 1998.

[50] C. Jong-Woo and S. Seung-Ki, "Fast current controller in three-phase AC/DC boost converter using d-q axis crosscoupling," *IEEE Transactions on Power Electronics,* vol. 13, pp. 179-185, 1998.

[51] L. Harnefors and H. P. Nee, "Model-based current control of AC machines using the internal model control method," *IEEE Transactions on Industry Applications,* vol. 34, pp. 133-141, 1998.

[52] X. Lie, B. R. Andersen, and P. Cartwright, "VSC transmission operating under unbalanced AC conditions - analysis and control design," *IEEE Transactions on Power Delivery,* vol. 20, pp. 427-434, 2005.

[53] P. Jiuping, N. Reynaldo, T. Le, and H. Per, "VSC-HVDC Control and Application in Meshed AC Network " in *IEEE-PES General meeting*, Pittsburggh, Pennsylvania, USA, 2008.

[54] D. Cuiqing, "VSC-HVDC for Industrial Power Systems," PhD Thesis, Electric Power Engineering, Chalmers University of Technology, Gothenburg, 2007.

[55] J. Beerten, S. Cole, and R. Belmans, "Generalized Steady-State VSC MTDC Model for Sequential AC/DC Power Flow Algorithms," *IEEE Transactions on Power Systems,* vol. 27, pp. 821-829, 2012.

[56] H. Temesgen, U. Kjetil, and U. Tore, "Control of Multiterminal HVDC Transmission for Offshore Wind Energy " in *Nordic Wind Power Conference 10 - 11.09.2009*, Bornholm, Denmark, 2009.

[57] L. Jun, O. Gomis-Bellmunt, J. Ekanayake, and N. Jenkins, "Control of multi-terminal VSC-HVDC transmission for offshore wind power," in *The 13th European Conference on Power Electronics and Applications, 2009. EPE '09*, Barcelona, Spain, 2009.

[58] X. Lie, Y. Liangzhong, and M. Bazargan, "DC grid management of a multi-terminal HVDC transmission system for large offshore wind farms," in *International Conference on Sustainable Power Generation and Supply, 2009. SUPERGEN '09*, Nanjing, China, 2009.

[59] R. da Silva, R. Teodorescu, and P. Rodriguez, "Power delivery in multiterminal VSC-HVDC transmission system for offshore wind power applications," in *Innovative Smart Grid Technologies Conference Europe (ISGT Europe), 2010*, Gothenburg, Sweden, 2010.

[60] P. Gustavo, "Operation of HVDC Grids in Parallel with AC Grids," Master Thesis, Department of Energy and Environment, Chalmers University of Technology, Gothenburg, Sweden, 2010.

[61] "HVDC Projects List, March 2012 - Existing or Under Construction " IEEE Transmission and Distribution Committee, [Online]. Available: http://www.ece.uidaho.edu/hvdcfacts/Projects/HVDCProjectsListingMarch2012-existing.pdf

[62] "HVDC Projects List, March 2012 - Planned," IEEE Transmission and Distribution Committee, [Online]. Available: http://www.ece.uidaho.edu/hvdcfacts/Projects/HVDCProjectsListingMarch2012-planned.pdf

[63] J. Wood and B. F. Wollenberg, *Power Generation Operation and Control*, Second Edition ed.: John Wiley and Sons, 1996.

[64] H. W. Dommel and W. F. Tinney, "Optimal Power Flow Solutions," *IEEE Transactions on Power Apparatus and Systems,* vol. PAS-87, pp. 1866-1876, 1968.

[65] B. Stott, O. Alsac, and A. J. Monticelli, "Security analysis and optimization," *Proceedings of the IEEE,* vol. 75, pp. 1623-1644, 1987.

[66] A. L'Abbate, G. Migliavacca, G. Fulli, C. Vergine, and A. Sallati, "The European research project REALISEGRID: Transmission planning issues and methodological approach towards the optimal development of the pan-European system," in *IEEE Power and Energy Society General Meeting, 2012*, San Diego, California, USA, 2012.

[67] R. de Dios, F. Soto, and A. J. Conejo, "Planning to expand?," *Power and Energy Magazine, IEEE,* vol. 5, pp. 64-70, 2007.

[68] S. de la Torre, A. J. Conejo, and J. Contreras, "Transmission Expansion Planning in Electricity Markets," *IEEE Transactions on Power Systems,* vol. 23, pp. 238-248, 2008.

[69] H. Singh, H. Shangyou, and A. Papalexopoulos, "Transmission congestion management in competitive electricity markets," *IEEE Transactions on Power Systems,* vol. 13, pp. 672-680, 1998.

[70] M. A. Abido, "Multiobjective evolutionary algorithms for electric power dispatch problem," *IEEE Transactions on Evolutionary Computation,* vol. 10, pp. 315-329, 2006.

[71] M. A. Abido, "Environmental/economic power dispatch using multiobjective evolutionary algorithms," *IEEE Transactions on Power Systems,* vol. 18, pp. 1529-1537, 2003.

[72] J. A. Momoh, "Optimal power flow with multiple objective functions," in *Proceedings of the Twenty-First Annual North-American Power Symposium*, 1989, pp. 105-108.

[73] Q. Zhifeng, G. Deconinck, and R. Belmans, "A literature survey of Optimal Power Flow problems in the electricity market context," in *IEEE PES Power Systems Conference and Exposition (PSCE), 2009*, Seattle, WA, USA, 2009.

[74] X. Yan, D. Zhao Yang, X. Zhao, Z. Rui, and W. Kit Po, "Power system transient stability-constrained optimal power flow: A comprehensive review," in *Power and Energy Society General Meeting, 2012 IEEE*, San Diego, California, USA, 2012.

[75] D. Gan, R. J. Thomas, and R. D. Zimmerman, "Stability-constrained optimal power flow," *IEEE Transactions on Power Systems,* vol. 15, pp. 535-540, 2000.

[76] Z. Wenjuan, L. Fangxing, and L. M. Tolbert, "Review of Reactive Power Planning: Objectives, Constraints, and Algorithms," *IEEE Transactions on Power Systems,* vol. 22, pp. 2177-2186, 2007.

[77] C. Lehmkoster, "Security constrained optimal power flow for an economical operation of FACTS-devices in liberalized energy markets," *IEEE Transactions on Power Delivery,* vol. 17, pp. 603-608, 2002.

[78] G. M. Huang and N. C. Nair, "Incorporating TCSC into the voltage stability constrained OPF formulation," in *Power Engineering Society Summer Meeting, 2002 IEEE*, Chicago, USA, 2002, pp. 1547-1552 vol.3.

[79] M. De, "Effect of congestion and voltage security on pricing in deregulated environment," in *TENCON 2008 - 2008 IEEE Region 10 Conference*, Hyderabad, India, 2008.

[80] R. S. Lubis, S. P. Hadi, and Tumiran, "Modeling of the generalized unified power flow controller for optimal power flow," in *2011 International Conference on Electrical Engineering and Informatics (ICEEI)*, Bandung, Indonesia, 2011, pp. 1-6.

[81] R. R. Shoults and D. T. Sun, "Optimal Power Flow Based Upon P-Q Decomposition," *IEEE Transactions on Power Apparatus and Systems,* vol. PAS-101, pp. 397-405, 1982.

[82] G. C. Contaxis, B. C. Papadias, and C. Delkis, "Decoupled Power System Security Dispatch," *IEEE Transactions on Power Apparatus and Systems,* vol. PAS-102, pp. 3049-3056, 1983.

[83] A. G. Bakirtzis and P. N. Biskas, "A decentralized solution to the DC-OPF of interconnected power systems," *IEEE Transactions on Power Systems,* vol. 18, pp. 1007-1013, 2003.

[84] R. Korab and G. Tomasik, "AC or DC OPF based LMP's in a competitive electricity market?," in *CIGRE/IEEE PES, 2005. International Symposium*, San Antonio, Teaxas, USA, 2005, pp. 61-68.

[85] J. A. Momoh, R. Adapa, and M. E. El-Hawary, "A review of selected optimal power flow literature to 1993. I. Nonlinear and quadratic programming approaches," *IEEE Transactions on Power Systems,* vol. 14, pp. 96-104, 1999.

[86] J. A. Momoh, M. E. El-Hawary, and R. Adapa, "A review of selected optimal power flow literature to 1993. II. Newton, linear programming and interior point methods," *IEEE Transactions on Power Systems,* vol. 14, pp. 105-111, 1999.

[87] M. Huneault and F. D. Galiana, "A survey of the optimal power flow literature," *IEEE Transactions on Power Systems,* vol. 6, pp. 762-770, 1991.

[88] D. W. Wells, "Method for economic secure loading of a power system," *Proceedings of the Institution of Electrical Engineers,* vol. 115, pp. 1190-1194, 1968.

[89] F. G. M. Lima, F. D. Galiana, I. Kockar, and J. Munoz, "Phase shifter placement in large-scale systems via mixed integer linear programming," *IEEE Transactions on Power Systems,* vol. 18, pp. 1029-1034, 2003.

[90] N. Grudinin, "Reactive power optimization using successive quadratic programming method," *IEEE Transactions on Power Systems,* vol. 13, pp. 1219-1225, 1998.

[91] A. Berizzi, M. Delfanti, P. Marannino, M. S. Pasquadibisceglie, and A. Silvestri, "Enhanced Security-Constrained OPF With FACTS Devices," *IEEE Transactions on Power Systems,* vol. 20, pp. 1597-1605, 2005.

[92] S. N. Talukdar, T. C. Giras, and V. K. Kalyan, "Decompositions For Optimal Power Flows," *IEEE Transactions on Power Apparatus and Systems,* vol. PAS-102, pp. 3877-3884, 1983.

[93] G. F. Reid and L. Hasdorff, "Economic Dispatch Using Quadratic Programming," *IEEE Transactions on Power Apparatus and Systems,* vol. PAS-92, pp. 2015-2023, 1973.

[94] R. C. Burchett, H. H. Happ, and D. R. Vierath, "Quadratically Convergent Optimal Power Flow," *IEEE Transactions on Power Apparatus and Systems,* vol. PAS-103, pp. 3267-3275, 1984.

[95] J. A. Momoh, "A generalized quadratic-based model for optimal power flow," in *IEEE International Conference on Systems, Man and Cybernetics, 1989*, Cambridge, Massachusetts, USA, 1989, pp. 261-271 vol.1.

[96] N. Karmarkar, "A New Polynomial-Time Algorithm for Linear Programming," in *The Sixteenth Annual ACM Symposium on Theory of Computing*, Washington. DC, USA, 1984.

[97] Y. Wei, Y. Juan, D. C. Yu, and K. Bhattarai, "A new optimal reactive power flow model in rectangular form and its solution by predictor corrector primal dual interior point method," *IEEE Transactions on Power Systems,* vol. 21, pp. 61-67, 2006.

[98] H. Wang, C. E. Murillo-Sanchez, R. D. Zimmerman, and R. J. Thomas, "On Computational Issues of Market-Based Optimal Power Flow," *IEEE Transactions on Power Systems,* vol. 22, pp. 1185-1193, 2007.

[99] A. G. Bakirtzis, P. N. Biskas, C. E. Zoumas, and V. Petridis, "Optimal power flow by enhanced genetic algorithm," *IEEE Transactions on Power Systems,* vol. 17, pp. 229-236, 2002.

[100] J. Yuryevich and W. Kit-Po, "Evolutionary programming based optimal power flow algorithm," *IEEE Transactions on Power Systems,* vol. 14, pp. 1245-1250, 1999.

[101] P. E. Onate Yumbla, J. M. Ramirez, and C. A. Coello Coello, "Optimal Power Flow Subject to Security Constraints Solved With a Particle Swarm Optimizer," *IEEE Transactions on Power Systems,* vol. 23, pp. 33-40, 2008.

[102] "GAMS - The Users' Guide," GAMS Development Corporation, Washington, DC, USA, July 2011.

[103] C. Cagigas and M. Madrigal, "Centralized vs. competitive transmission expansion planning: the need for new tools," in *Power Engineering Society General Meeting, 2003 IEEE*, Toronto, Canada, 2003, p. 1017 Vol. 2.

[104] G. Latorre, R. D. Cruz, J. M. Areiza, and A. Villegas, "Classification of publications and models on transmission expansion planning," *IEEE Transactions on Power Systems,* vol. 18, pp. 938-946, 2003.

[105] M. R. Hesamzadeh, N. Hosseinzadeh, and P. J. Wolfs, "Economic assessment of transmission expansion projects in competitive electricity markets - an analytical review," in *43rd International Universities Power Engineering Conference (UPEC), 2008*, 2008.

[106] J. Hicks, "The Foundations of Welfare Economics," *Economic Journal,* 1939.

[107] B. Williams, "Cost-benefit analysis," *Economic & Labour Market Review* vol. 2, December 2008.

[108] "Guideline for Cost Benefit Analysis of Grid Development Projects," ENTSO-E, Tech. Rep., December 2012.

[109] K. Bhattacharya, M. Bollen, and J. Daalder, *Operation of Restructured Power System*: Kluwer Academic Publishers, 2001.

[110] G. Daelemans, "VSC HVDC in meshed networks," Master Thesis, Katholieke Univiersity Leuven, Leuven, Belgium, 2008.

[111] Z. Xiao-Ping, "Multiterminal voltage-sourced converter-based HVDC models for power flow analysis," *IEEE Transactions on Power Delivery,* vol. 19, pp. 1877-1884, 2004.

[112] "GAMS - The Solver Manuals," GAMS Development Corporation, Washington, DC, USA, July 2012.
[113] *Power World webpage*. Available: http://www.powerworld.com/
[114] K. Walve, "Nordic32A - A Cigre test system for simulation of transient stability and long term dynamics," Svenska Kraftnät, Sweden, Tech. Rep., 1994.
[115] C. Grigg, P. Wong, P. Albrecht, R. Allan, M. Bhavaraju, R. Billinton, Q. Chen, C. Fong, S. Haddad, S. Kuruganty, W. Li, R. Mukerji, D. Patton, N. Rau, D. Reppen, A. Schneider, M. Shahidehpour, and C. Singh, "The IEEE Reliability Test System-1996. A report prepared by the Reliability Test System Task Force of the Application of Probability Methods Subcommittee," *IEEE Transactions on Power Systems,* vol. 14, pp. 1010-1020, 1999.
[116] "The Energy Market 2004," Swedish Energy Agency, 2004.
[117] (2011, May). *Nord Pool Spot*. Available: http://www.nordpoolspot.com/Market-data1/Power-system-data/Consumption1/Consumption/ALL/Hourly1/
[118] G. Daelemans, K. Srivastava, M. Reza, S. Cole, and R. Belmans, "Minimization of steady-state losses in meshed networks using VSC HVDC," in *Power & Energy Society General Meeting, 2009.*, Calgary, Canada, 26-30 July 2009.
[119] R. Mohaned, "Evaluation of HVDC Light as an alternative for the Vancouver Island transmission reinforcement (VITR) project, Appendix Q," TransGrid Solutions Inc.Tech. Rep., 2005.
[120] "Projected Costs of Generating Electricity," International Energy Agency (IEA), Tech. Rep., 2010.